

Review

Bohdan Volynets, Farhad Ein-Mozaffari and Yaser Dahman*

Biomass processing into ethanol: pretreatment, enzymatic hydrolysis, fermentation, rheology, and mixing

DOI 10.1515/gps-2016-0017

Received February 18, 2016; accepted June 22, 2016; previously published online October 14, 2016

Abstract: Alternate energy resources need to be developed to amend for depleting fossil fuel reserves. Lignocellulosic biomass is a globally available renewable feedstock that contains a rich sugar platform that can be converted into bioethanol through appropriate processing. The key steps of the process, pretreatment, enzymatic hydrolysis, and fermentation, have undergone considerable amount of research and development over the past decades nearing the process to commercialization. In order for the commercialization to be successful, the process needs to be operated at high dry matter content of biomass, especially in the enzymatic hydrolysis stage that influences ethanol concentration in the final fermentation broth. Biomass becomes a thick paste with challenging rheology for mixing to be effective. As the biomass consistency increases, yield stress increases which limits efficiency of mixing with conventional stirred tanks. The purpose of this review is to provide features and perspectives on processing of biomass into ethanol. Emphasis is placed on rheology and mixing of biomass in the enzymatic hydrolysis step as one of the forefront issues in the field.

Keywords: ethanol; lignocellulose; mixing; pretreatment; rheology.

1 Current outlook

Growing energy demand and increasing concern for the security of supply of oil tied with the urge to reduce greenhouse gas emissions have led to countries such as

the US and European Union (EU) to set targets for replacing petroleum fuels with renewable biofuels. The US Department of Energy has set a goal for supplying 30% of the gasoline demand with biofuels by 2030, and the EU projects 10% of its transportation fuels to be derived from biofuels by 2020 [1]. Bioethanol made from sugar (Brazil) or starch (the US) is the most common renewable biofuel today [2]. It is a known substitute to gasoline or an additive to gasoline [3]. Such fuels derived from crops are termed first-generation biofuels. However, using crops for fuel production competes with food and is a short-term solution due to limited availability of land. Therefore, alternative renewable sources of energy such as lignocellulosic biomass will need to be pursued to provide for the shortage in first-generation biofuels. Biofuels derived from lignocellulose (neutral with respect to production of greenhouse gasses) are second-generation biofuels, research into which has escalated over the past decade with a number of pilot plants operating throughout the world [3–5].

Lignocellulose is the primary component of plant biomass and is available in abundance from various renewable feedstock such as agricultural residues (corn stover, wheat straw, sugarcane bagasse), dedicated energy crops (switch grass, poplar trees), forestry residues (wood chips, sawdust) and municipal solid waste [6]. Overall, global lignocellulosic biomass potential is between 10 and 50×10^9 tons per year [7]. Global bioethanol potential of agriculture residues is presented by [8]. Data were collected using FAOSTAT statistical software. Average values were obtained for years between 1997 and 2001. Results are shown in Table 1. Ground cover of 60% is applied to every residue for the exception of rice straw and sugarcane bagasse. Rice straw, wheat straw, and corn stover are the top three crop residues in the world. Corn (42%) is the predominant crop in North America. Rice (90%) and wheat (43%) dominate in Asia. Wheat also dominates among the crops in Europe (32%). In total, crop residues could replace 28.6% of global gasoline consumption. Mediterranean Basin annual production of lignocellulosic residues

*Corresponding author: Yaser Dahman, Department of Chemical Engineering, Ryerson University, Toronto, Ontario M5B 2K3, Canada, e-mail: ydahman@ryerson.ca

Bohdan Volynets and Farhad Ein-Mozaffari: Department of Chemical Engineering, Ryerson University, Toronto, Ontario M5B 2K3, Canada

Table 1: Annual availability and bioethanol potential of agriculture residues [8].

Crop residue	Availability (Tg/annum)	Bioethanol potential (GL)
Corn stover	203.6	58.6
Barley straw	58.5	18.1
Oat straw	10.6	2.78
Rice straw	731.3	204.6
Wheat straw	354.4	103.8
Sorghum straw	10.32	2.8
Sugarcane bagasse	180.7	51.3
Total	1549.4	442.0

is around 180 Mton, which can yield 60 Mtoe (Mton oil equivalent) of ethanol [9].

Conversion of biomass to ethanol includes (1) pretreatment, (2) enzymatic hydrolysis, (3) fermentation, and (4) distillation [10]. Pretreatment sometimes includes mechanical size reduction which must be followed by a strong thermochemical pretreatment to break up lignocellulosic structure solubilizing hemicellulose and/or lignin to make cellulose more accessible to hydrolytic enzymes. Enzymatic hydrolysis releases glucose from cellulose for ethanol fermentation. The two steps can be done together in a single step called simultaneous saccharification and fermentation (SSF). Typical biomass-to-ethanol process flowsheet is shown in Figure 1. Using lignin as a solid fuel can cover with an excess all steam and electricity requirements of the process making it a very valuable by-product [4].

In order to obtain high ethanol concentration for distillation in lignocellulosic biorefinery process, steps such as enzymatic hydrolysis or SSF need to be operated at high solid loading. It is estimated that solids loading of around 30% (w/w) is required to obtain ethanol concentration in the final fermentation broth up to 5%–10% (w/w) [4, 11]. Operating ethanol production process at high solids loading has its advantages. Reduced use of water means

lower capital costs and lower energy consumption during distillation. However, at high solids loading transport, limitations for the enzymes become significant to a point where mixing of biomass has become one of the primary issues in the area of lignocellulosic ethanol. At high solids loading (>15%, w/w), biomass possesses complex rheological characteristics that affect mixing energy consumption. As such, mixing in conventional stirred tanks becomes too costly and inefficient in terms of distributing the enzymes throughout the biomass. Alternate reactor geometries are ultimately required to achieve the goal of low power consumption and high transport efficiency. These can be helical ribbon or rotating drum bioreactors.

2 Biomass structure and composition

Lignocellulosic biomass consists of 33%–55% cellulose, 13%–33% hemicellulose, and 13%–32% lignin by dry weight (Table 2). These three main components constitute up to 90% of biomass with the remaining mass being attributed to ash, structural proteins, and extractives [24]. Cellulose and hemicellulose are a source of C6 and C5 sugars for bacterial fermentation. Hemicelluloses can contain pentoses and hexoses, small amounts of uronic acids, and hydroxyl groups and are partially substituted by acetyl groups (0.5%–3.9%). Xylan is the major component of hemicellulose in agriculture residues and hardwoods, while softwood hemicelluloses contain a substantial ratio of mannan (up to 50%) [25]. Lignin consists of aromatic *p*-hydroxyphenyl (H), guaiacyl (G) and syringyl (S) units varying in amount depending on biomass type [26].

Cellulose consists of linear β -(1,4)-linked D-glucopyranose chains. The chains are arranged by hydrogen bonding into 3×5 nm diameter microfibrils that are in turn arranged into macrofibrils 50–250 nm in diameter [27]. In pretreated biomass cellulose chains

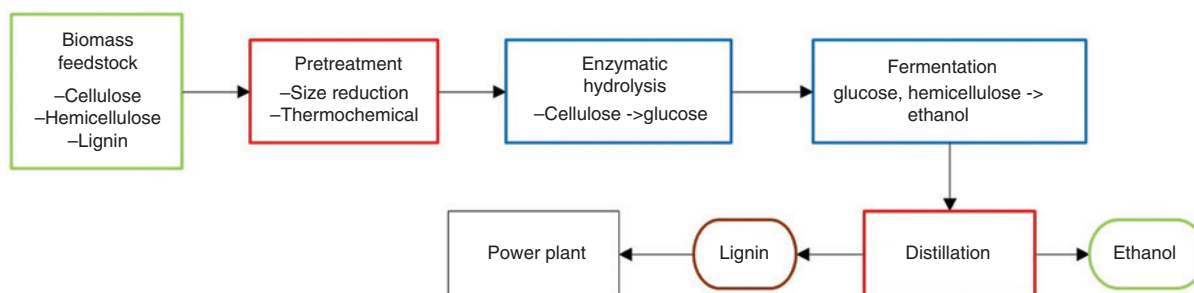
**Figure 1:** Typical bioethanol production flowsheet.

Table 2: Chemical composition of various biomasses.

Biomass	Cellulose (%, w/w)	Hemicellulose (%, w/w)	Lignin (%, w/w)	Reference
Agriculture residues				
Corn stover	35–37	20–31	18–23	[12, 13]
Wheat straw	33–40	20–25	15–20	[6]
Rice straw	36–49	22–33	16–17	[14, 15]
Barley straw	34–36	23–29	13–23	[16, 17]
Bagasse	33–41	23–31	14–23	[18]
Energy crops				
Switchgrass	35–39	29–31	18–32	[19, 20]
Poplar trees	39–46	18–19	20–25	[21]
Forestry residues				
Hardwoods	46–55	13–18	22–27	[22]
Municipal solid waste				
Paper pulp	60–70	10–20	5–10	[23]

contain a reducing end and a non-reducing end. Structurally, cellulose microfibrils are covered with a heterogeneous hemicellulose polymer which is wrapped by amorphous lignin polymer that makes biomass resistant to chemical or biological catalyst. Lignin-carbohydrate complexes play a major role in biomass recalcitrance. They are the bridges between lignin and hemicelluloses formed via ester and ether bonds between *p*-coumaric and ferulic acids [26]. Recalcitrant structure of plant cell wall is

depicted in Figure 2. Processing of lignocellulose into bio-fuels must involve a strong thermochemical pretreatment to disrupt the recalcitrant lignocellulosic matrix making cellulose microfibrils accessible to enzymes [13, 14, 18].

Genetic manipulation of plants to reduce lignin content can make them more favorable for bioprocessing [28, 29]. Down-regulation of the switchgrass coffeic acid *O*-methyl transferase gene reduces thermal-chemical, enzymatic, and microbial recalcitrance of the plant. The manipulation reduces the syringyl:guaiacyl lignin monomer ratio and lignin content. It is reported that the down-regulated switchgrass requires less severe pretreatment and 300%–400% lower cellulose dosages and increases ethanol yield by up to 38% [29]. Through overexpression of the transcription factor PvMYB4 which reduces carbon deposition into lignin and phenolic fermentation inhibitors, Shen et al. [30] was able to increase ethanol yield from switchgrass by 2.6-fold. Down-regulation of 4-coumarate coenzyme A ligase, a major lignin synthesis enzyme, decreased lignin content by 45% and increased cellulose fraction by 15% in genetically modified aspen without harmful effects on plant growth, development or structural integrity [7]. Engineering vascular bundles and pits between connecting cell walls to improve penetration of chemical and enzymes into biomass fragments could be one of the future trends aimed at improving transport limitations during processing of lignocellulose [31].

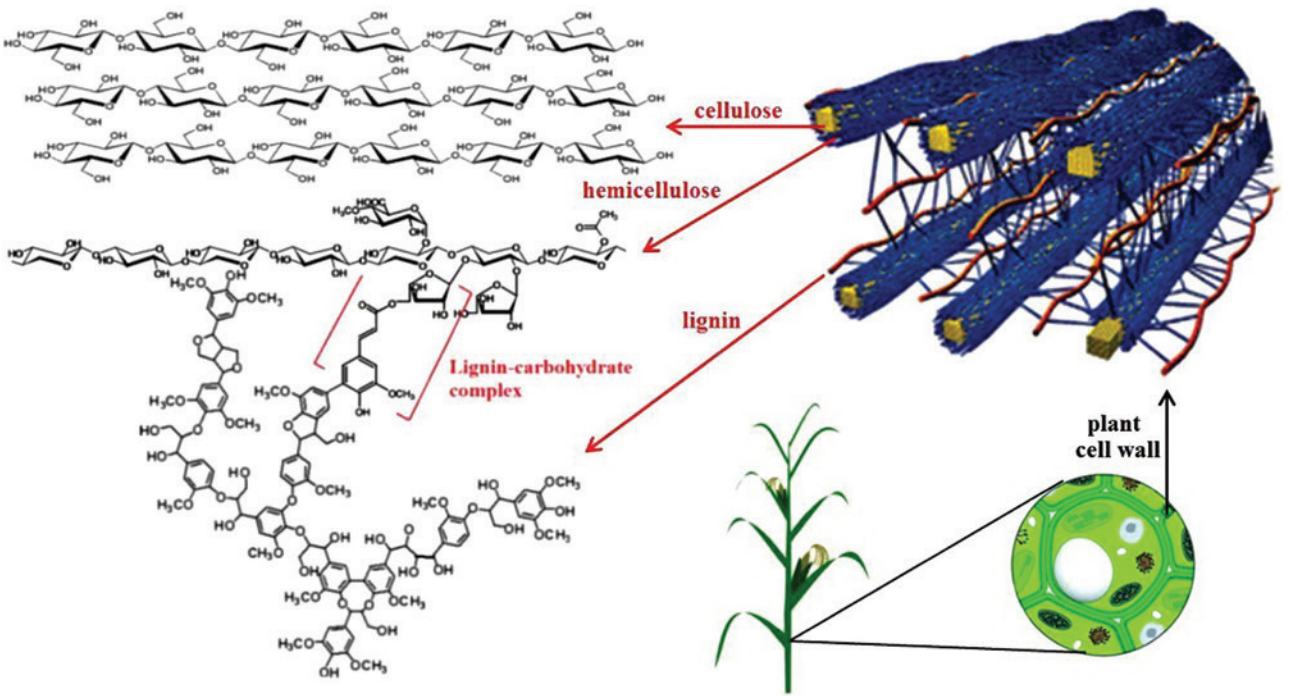


Figure 2: Structure of lignocellulose.

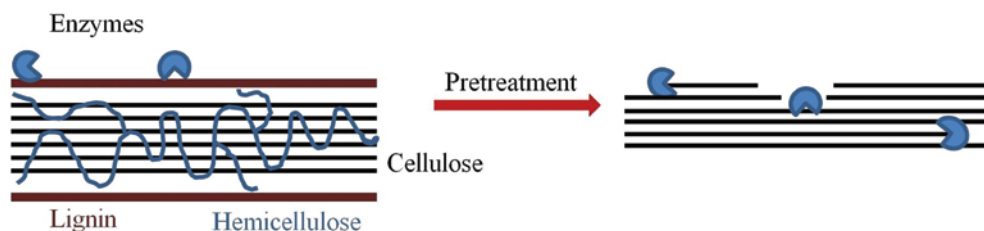


Figure 3: Pretreatment enhances accessibility of cellulose to enzymes.

3 Pretreatment

The need for pretreatment in lignocellulose-to-ethanol production process is unprecedented. For instance, the conversion of cellulose to glucose after enzymatic hydrolysis of corn stover following steam explosion pretreatment increased more than four times compared to untreated material [32]. Without pretreatment, too much enzyme is required to saccharify biomass making the process unfeasible [5]. Figure 3 depicts the concept of enhanced accessibility of cellulose to enzymes due to a pretreatment. Pretreatments are categorized into mechanical, acidic, alkali, oxidative, fractionative, and biological. Optimal pretreatment conditions with respect to glucose yields for various thermochemical pretreatments are shown in Table 3. Structural changes to biomass during mechanical and thermochemical pretreatments are shown in Figure 4.

3.1 Mechanical

Particle size reduction increases specific surface area and reduces crystallinity to improve accessibility of biomass to chemical and biological catalyst. It can take the form of knife milling [52], hammer milling [53] or ball or wet disk milling [54]. Mechanical pretreatment alone cannot be used as an effective pretreatment option for biomass processing due to high specific energy consumption. It is rather used as an additional step prior to physiochemical pretreatments. However, due to high energy consumption, some pilot plants limit this pretreatment to coarse cutting in the case of wheat straw [4]. Particle size reduction to pieces 1–15 cm in length would be ideal for future ethanol biorefineries to circumvent high energy demand of mechanical comminution [31]. If smaller particle size is otherwise required, knife milling can be followed by hammer milling.

Table 3: Optimum pretreatment conditions of various thermochemical pretreatments.

Pretreatment	Pretreatment conditions	EH yield ^a (%)	Feedstock	References
Steam explosion	220–230°C, 2–4 min	90	Hardwood	[33]
	195°C, 4.5 min, 4.5% SO ₂	87	Softwood	[34]
	200°C, 5 min, 2% H ₂ SO ₄	84	Corn stover	[32]
Dilute acid	162°C, 9.8 min, 0.8% H ₃ PO ₄	75	Corn stover	[35]
	170°C, 4.4 min, 1% H ₂ SO ₄	99	Corn stover	[36]
	179°C, 50 min, 46 mM maleic acid	85	Wheat straw	[37]
Hydrothermal	190°C, 15 min	90	Corn stover	[38]
Lime	100°C, 15 min, 0.1 g Ca(OH) ₂ /g of dry biomass	87	Coastal Bermuda grass	[39]
	55°C, 4 weeks, aeration	93	Corn stover	[40]
NaOH	190°C, 30 min, 0.3 g NaOH/g of dry biomass, microwave	99	Switchgrass	[41]
	190°C, 30 min, 0.3 g NaOH/g of dry biomass	92	Switchgrass	[41]
	121°C, 60 min, 1.0% NaOH	90	Wheat straw	[42]
NH ₃	69°C, 14 h, 20% aqueous NH ₃	60	Rapeseed straw	[43]
AFEX	90°C, 5 min, 1 g NH ₃ /g biomass, 17–20.4 atm	91	Corn stover	[44]
Wet oxidation	195°C, 15 min, 12 bar O ₂ , 2 g/l Na ₂ CO ₃	85	Corn stover	[45]
Ozonolysis	Ozone	89	Wheat straw	[46]
Alkaline H ₂ O ₂	23°C, 48 h, 0.5 g H ₂ O ₂ /g biomass, 5 M NaOH	95	Corn stover	[47]
Ionic liquid	160°C, 3 h [C ₂ mim][OAc] ^b	96	Switchgrass	[48]
Phosphoric acid	50°C, 85% H ₃ PO ₄ , 30 min	96	Corn stover	[49]
Organosolv	180°C, 0 min, 1:1 ethanol:water, 1% H ₂ SO ₄	76	Pitch pine	[50]
Supercritical CO ₂	165°C, 30 min, 210.9 atm	85	Aspen	[51]

^aGlucose yield after enzymatic hydrolysis (EH). ^bIon pairs of the ionic liquid [C₂mim][OAc]: carbon atom C₂ of the [C₂mim]⁺ cation and oxygen atom O of the [OAc][−] anion.

Mechanical	Thermochemical			
	Acidic	Alkali	Oxidative	Fractionative
Cutting Milling <u>Ball milling</u> – Particle size reduction <u>– Reduction in crystallinity index</u>	Dilute acid Liquid hot water <u>Steam explosion</u> – Hemicellulose hydrolysis – Increase in biomass porosity – Production of acetic acid <u>– Separation of fibres</u>	Lime NaOH Ammonia APEX – Delignification – Swelling of biomass – Removal of hemicellulose – Deacetylation <u>– Lignin fragmentaion</u>	Wet oxidation Ozonolysis <u>Alkali peroxide</u> – Delignification – Hemicellulose solubilization <u>– Swelling of biomass</u>	Phosphoric acid Ionic liquids – Cellulose dissolution – Reduction in crystallinity index Organosolv – Removal of lignin – Removal of hemicellulose

Figure 4: Structural changes during pretreatments of biomass. (Underlined features are additional information pertaining to underlined pretreatments only).

Fine mechanical comminution is applied prior to all thermochemical pretreatments in Table 3 to eliminate particle size as a factor in studying enzymatic hydrolysis yields.

3.2 Acidic

3.2.1 Steam explosion

Steam explosion pretreatment involves pressurizing biomass at high temperature followed by a rapid decompression. Steam explosion solubilizes hemicellulose into monomers, changes lignin structure precipitating it onto biomass, and causes separation of fibers. It is effective without a catalyst but can also be SO_2 and H_2SO_4 catalyzed to improve hemicellulose dissolution [32–34]. Recently, Yu et al. [55] have developed a new steam explosion device composed of a cylinder and a piston that completes the explosion within 0.0875 s which is 123 times faster when compared to conventional valve release vessels. Advantages include high hemicellulose solubilization and production of a porous substrate that is easily hydrolyzed into sugars. Also, lignin is transformed in structure into liquid state and precipitates back onto biomass. At the end of enzymatic hydrolysis, transformed lignin is used as a solid fuel in local power plants.

3.2.2 Dilute acid

Pretreatment with dilute sulfuric, phosphoric, or organic acids solubilizes hemicellulose from biomass. A drawback is that some of the resulting sugars are degraded to known fermentation inhibitors furfural and hydromethylfurfural requiring a detoxification step. However, cellulose digestibility following the pretreatment is high (75%–100%) [18, 35–37], which makes it another widely used pretreatment option.

3.2.3 Hydrothermal

Pretreatment with liquid hot water solubilizes hemicellulose with internally produced acids such as acetic acid (autohydrolysis) during the pretreatment. Advantages include minimal production of fermentation inhibitors and reduced use of chemical for pH adjustment [13, 38].

3.3 Alkali

3.3.1 Lime

Lime pretreatment of biomass is performed at mild conditions but at longer reaction times compared to other pretreatments to remove lignin [39, 40, 56]. The pretreatment can be operated at oxidative conditions using air to enhance lignin removal. At these conditions, lignin removal can reach up to 88% compared to 50% at non-oxidative conditions [40]. Xylose yield can range between 70 and 80% [39, 40].

3.3.2 NaOH

Pretreatment with NaOH is optimal at high temperatures and long reaction time. Microwave can be used to further improve disruption of lignocellulosic matrix [41]. Delignification ranges between 33 and 72% depending on reaction conditions [42]. Xylose yield ranges between 90 and 99% [41, 42].

3.3.3 NH_3

Soaking in aqueous ammonia (SAA) at mild temperatures removes around 50% lignin, while all of cellulose and

xylan remain in solids. The pretreatment suffers from low glucose digestibility most likely linked to lower lignin removal compared to other alkali pretreatments [43]. Also, because xylan remains in solids, it blocks the access of enzymes to the substrate.

3.3.4 Ammonia fiber expansion

During ammonia fiber expansion (AFEX) process, biomass is treated with liquid anhydrous ammonia at mild temperatures and high pressure followed by a rapid decompression. As a result, biomass swells including lignin solubilization, cellulose decrystallization, and hemicellulose hydrolysis. Xylose yield was found to be 80% [44]. The pretreatment is quite economical as described in following sections. This pretreatment is unique in that it fragments lignin into small blocks without destruction of lignin polymer chemical structure implied as solubilization in other pretreatments.

3.4 Oxidative

3.4.1 Wet oxidation

Wet oxidation solubilizes 30%–55% lignin and 60%–80% hemicellulose, while over 90% cellulose remains in the solid fraction. The process takes place in high atmosphere oxygen environment with an alkali catalyst (Na_2CO_3) [45, 57]. High capital cost of pressurized equipment is a big disadvantage of this process.

3.4.2 Ozonolysis

Ozone oxidizes C=C bonds in lignin polymer, releasing soluble compounds such as formic and acetic acid. The pretreatment is more effective for feedstock lower in lignin content. Up to 30% of acid insoluble lignin is removed by the process [46]. Up to 17% of both xylan and glucan are also solubilized [58]. Loss of carbohydrate components during ozone pretreatment is too high to be a viable option.

3.4.3 Alkaline hydrogen peroxide

Alkaline H_2O_2 pretreatment solubilizes lignin and xylan as well as causes swelling of biomass [59, 60]. The pretreatment is performed at room temperature but at

pretreatment time of days. Instability of H_2O_2 and large production of salt after pH adjustment can be disadvantageous [47]. Long pretreatment times would mean that a lot of capital would be involved in handling tonnages of daily feed. Also, production of salts can hurt the fermentation process.

3.5 Fractionative

3.5.1 Ionic liquids

Pretreatment with ionic liquids dissolves biomass into its constituent components. Upon addition of an anti-solvent such as water, the regenerated biomass contains cellulose in amorphous form that is highly susceptible to enzymatic hydrolysis. Recycling of the ionic liquid is nearly quantitative. Enzymatic hydrolysis yield depends on the ionic liquid used [48, 61, 62]. The price of an ionic liquid is currently too high for this pretreatment to be economic.

3.5.2 Phosphoric acid

Pretreatment with concentrated phosphoric acid (~85% w/w) takes place at low temperatures with the use of organic solvent (ethanol or acetone) to quench the reaction and precipitate dissolved cellulose and hemicellulose. Lignin is dissolved into the liquid phase and can be removed by washing out phosphoric acid with the organic solvent. A distiller is required to evaporate the solvent [49, 63]. This is a great pretreatment for a lignocellulose-based biorefinery where biomass components are fractionated.

3.5.3 Organosolv

Organosolv pretreatment utilizes organic solvent with or without an acid catalyst as delignification agent. Lignin is separately precipitated as a solid material, and carbohydrates are isolated as syrup. The pretreatment results in significant reduction in the degree of crystallinity of cellulose and solubilization of hemicellulose [64, 65]. However, glucose yields are on the lower side (~70%–75%) [50, 66].

3.6 Supercritical CO_2

Supercritical CO_2 pretreatment causes explosion of biomass which reduces cellulose crystallinity by about 50% and increases biomass porosity. Biomass has to be

pre-wetted in water prior to pretreatment. Dissolution of CO_2 in water increases acidity inside the reactor which causes auto-hydrolysis of hemicellulose [67]. The cost of CO_2 is low; however, the process requires high-pressure equipment for operation. The pretreatment was showed to be much more effective for hardwoods than softwoods [51]. Glucose yields for pretreated switch grass and corn stover were also very low [68].

3.7 Biological

White-rot fungi delignify biomass by producing lignin-degrading enzymes such as manganese peroxidase and lignin peroxidase [69]. Although it is an environmentally friendly process that does not involve the use of chemicals, several issues pertain: carbohydrate loss to sustain microbial growth, reactor scaling, heat build-up, and process control [70]. Bak et al. [51] obtained 64.9% glucose yield after enzymatic hydrolysis of rice straw pretreated with *Phanerochaete chrysosporium* for 15 days. Keller et al. [71] obtained 35.7% digestibility after pretreatment with *Cyathus stercoreus* for 29 days. Lengthy pretreatment times and lower digestibilities compared to other pretreatments are other issues that add up to the process. However, development of more aggressive microbial strains can yield improvements in the future for development of low-scale plants.

3.8 Additional considerations

Being the first step, pretreatment is the key step in ethanol biorefinery that affects downstream processes. An ideal pretreatment would have to satisfy the following criteria:

1. Low loss of carbohydrate platform. Feedstock cost can be as high as 50% of the overall ethanol selling price [72]. Loss of feedstock sugars could thus be detrimental to the overall process economics.
2. High cellulose and hemicellulose digestibility. Although most studies are focused on glucan yields, xylose can also be converted to ethanol by modern strains, and enzymes exist that can convert xylan to xylose.
3. Lignin utilization. Lignin can be used as fuel or as a platform for value-added chemicals. Either ways it is a major part of biomass composition, and its loss during pretreatment could be detrimental to the overall process economics.
4. Production of little or no fermentation inhibitors. An additional detoxification step could be

required entailing additional capital and operational expenses.

5. Minimize use of chemicals. Use of chemical acids or bases requires pH adjustment which could result in production of a lot of salts which could damage fermenting bacteria.
6. Operation at high solids loading. Some pilot plants operate at biomass loading of 15%–20% (w/w) [5] or even up to 40% (w/w) [4].

3.9 Economic considerations

Economic viability is the main obstacle to commercialization of lignocellulosic ethanol. Tao et al. [72] evaluated six pretreatment technologies for conversion of switchgrass into cellulosic ethanol: AFEX, dilute acid (DA), lime, liquid hot water (LHW), SAA, and SO_2 impregnated steam explosion (SO_2). Plant size was 2000 metric tons per day. EH was evaluated at solid content of 20% (w/w), and the slurry is then fermented by glucose-xylose fermenting bacteria. Solids from distillation are combusted to cover steam and electricity needs. Excess electricity is sold to the grid. Minimum ethanol selling price (MESP) is correlated with monomeric glucose and xylose yields. SAA pretreatment was found to have the highest MESP. SO_2 pretreatment resulted in highest monomeric sugar yields. However, MESP for SO_2 pretreatment was lower than AFEX and DA pretreatments due to costs associated with using SO_2 . LHW pretreatment produced significant amounts of unfermentable sugar oligomers which reflected on its higher MESP. MESP ranged between \$2.74/gal for AFEX pretreatments to \$4.07/gal for SAA pretreatment. AFEX pretreatment was followed by DA and SO_2 pretreatments in the range \$2.50–3.00/gal. Lime and LHW pretreatments were following in the range \$3.00–3.50/gal. Some 45%–53% of MESP for all six cases was attributed to feedstock cost. Total capital cost was in the range \$325–385M.

Kazi et al. [73] evaluated four pretreatment technologies: DA, two-stage DA, AFEX, and LHW; as well as three post-treatment scenarios: pervaporation, separate glucose and xylose fermentation, and on-site enzyme production. DA and AFEX pretreatments were the most feasible with ethanol production cost of \$1.36 and \$1.47/l of gasoline equivalent (LGE). LGE is the amount of ethanol equivalent in energy content to 1 l of gasoline. LHW and two-stage DA pretreatments were at \$1.77 and \$1.75/LGE, respectively. Substituting beer column with a pervaporation membrane was found to increase the present value of ethanol by \$0.14/LGE due to high capital cost of the membrane. Similarly, due to significant amount of feedstock being

Table 4: Total capital investment evaluated by different studies (plant capacity 2000 t/day).

Pretreatment	Total capital (\$MM, [72])	Total capital (\$MM, [74])	Total capital (\$MM, [73])
AFEX	348	212	386
DA	349	209	376
Lime	385	164	n.a.
LHW	325	201	327
Ammonia	364	211	n.a.
SO ₂	340	n.a.	n.a.
Two-stage DA	n.a.	n.a.	391

n.a., not available.

diverted to on-site enzyme production (9.2% of hydrolysis feedstock), this scenario resulted in \$0.06/LGE increase in present value compared to \$0.28/LGE for the base case (i.e. without the on-site enzyme production). The present value of separate glucose and xylose fermentation was \$0.11/LGE higher than the base case due to increased operating and capital costs for separate fermentation vessels and lower concentrations of ethanol in the beer columns.

Eggeman and Elander [74] evaluated five pretreatment technologies for bioprocessing of corn stover into ethanol: DA, LHW, AFEX, ammonia recycle percolation (ARP), and lime. Plant capacity was 2000 metric tons per day. Lime pretreatment had the lowest total fixed capital per gallon annual capacity, \$3.35/gal, followed by DA and AFEX at \$3.72/gal, and ARP and LHW at \$4.56 and \$4.57/gal, respectively. However, MESP for DA pretreatment was the lowest at about ~\$1.35/gal followed by AFEX at ~\$1.45/gal, and lime, ARP, and LHW at ~\$1.65/gal. The MESP of an ideal pretreatment was evaluated at ~\$1.00/gal. Compared to other studies, the total capital evaluated is on the order of \$100 M lower. Pretreatment capital is in the range of \$5–28 M which is much lower compared to pretreatment capital evaluated by Tao et al. [72], \$20–57 M. Total capital costs for different pretreatments are shown in Table 4.

4 Enzymatic hydrolysis

Cellulolytic or cellulase enzymes consist of three main groups of enzymes: exo-1,4- β -D-glucanases (EC 3.2.1.91), endo-1,4- β -D-glucanases (EC 3.2.1.4), and β -glucosidases (EC 3.1.1.21). Exoglucanases hydrolyze cellobiose units off of cellulose chains. They are divided into two forms – cellobiohydrolase I (CBH I) and II (CBH II). CBH I hydrolyzes cellulose chain from the reducing end, and CBH II proceeds from the non-reducing end [75]. Endoglucanases

randomly hydrolyze internal O-glycosidic bonds in cellulose chains resulting in oligomers of different lengths. β -glucosidases hydrolyze cellobiose to produce glucose [76, 77].

Hemicellulolytic or hemicellulase enzymes include endo-1,4- β -xylanase (EC 3.2.1.8) that hydrolyzes internal bonds in the xylan chain producing xylooligomers, exo-1,4- β -xylosidase (EC 3.2.1.37) that hydrolyzes xylooligomers releasing xylose, endo-1,4- β -mannase (EC 3.2.1.78) that hydrolyzes internal bonds in the mannan chain producing mannan oligomers, and exo-1,4- β -mannosidase (EC 3.2.1.25) that hydrolyzes mannoooligomers and mannobiose into mannose. Hemicellulose side groups are hydrolyzed by α -L-arabinofuranosidase (EC 3.2.1.99), endo- α -1,5-arabinanase (EC 3.2.1.99), α -glucuronidase (EC 3.2.1.139), α -galactosidase (EC 3.2.1.22), endo-galactanase (EC 3.2.1.89), acetyl xylan esterase (EC 3.1.1.72), acetyl mannan esterase (EC 3.1.1.6), and ferulic and *p*-cumaric acid esterases (EC 3.1.1.73) [78].

Enzymes act in synergy to hydrolyze biomass into sugars [79]. Zhang et al. [80] found that without β -glucosidase, the yield of glucose was 57.1%, which increased to 80% after addition of 2.9 mg protein/g glucan of β -glucosidase. Supplementation of 0.67 mg protein/g glucan of xylanase increased glucose and xylose yields by 6.5% and 26.5% respectively. Some 0.12 mg protein/g glucan of pectinase increased glucose and xylose yields by 7.5% and 29.3%, respectively. Selig et al. [81] found that there was 84.6% synergistic improvement in cellobiose release by addition of commercial xylanase (XynA) and two esterases (Axel and FaeA) activities. Synergistic improvement in xylobiose release was found to be 180.7%. Data on enzyme synergy is important for creating more potent enzyme cocktails. The diverse enzyme system is shown in Figure 5. Ye et al. [82] used genetic engineering such as cloning and expression to produce a bifunctional enzyme from hyperthermophilic bacterium *Caldicellulosiruptor bescii*. This enzyme is able to hydrolyze both cellulose and mannan oligosaccharides as well as show a modest synergistic effect with other endoglucanases.

4.1 Factors affecting enzymatic hydrolysis

Structural features of pretreated biomass substrate have a direct impact on enzymatic hydrolysis of lignocellulose. Lignin content and crystallinity index have the greatest effect, while acetyl content has a minor impact [83, 84]. Amorphous cellulose provides greater surface area for the action of enzyme than crystalline cellulose, thus the impact of crystallinity index. Acetyl

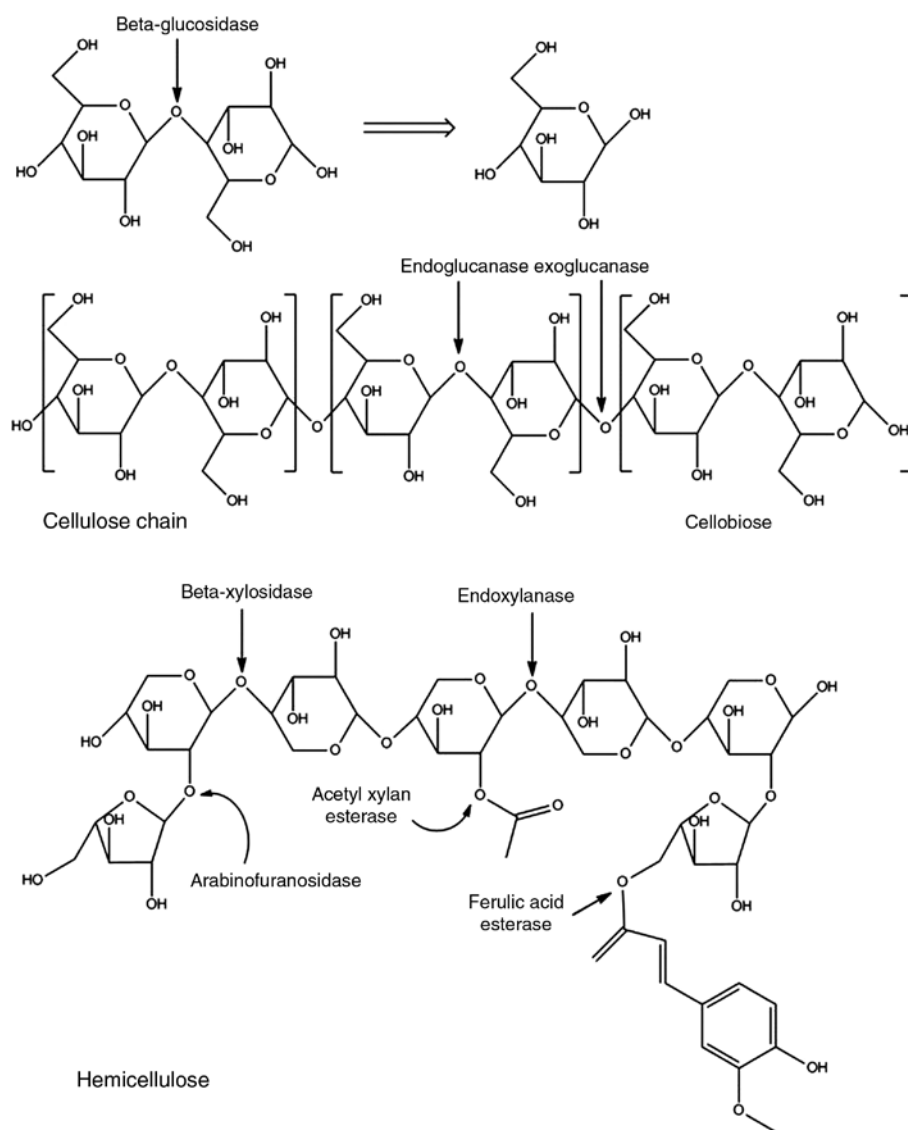


Figure 5: The enzyme system.

groups, hemicellulose, and lignin act as structural barrier, and lignin also affects the hydrolysis by unproductive binding of enzymes to lignin. Zhu et al. [83] also found that at short hydrolysis times, lignin content did not have a great effect when crystallinity was low, and at long hydrolysis times, crystallinity did not have as much of an effect when lignin content was low. Enzymes are affected by end-product inhibition by glucose and cellobiose. O'Dwyer et al. [85] investigated inhibition pattern for cellulose system at excess exoglucanase loading and found that sugar conversion is linearly proportional to the logarithm of enzyme loading. End-product inhibition becomes an issue at high biomass solids loading. Exoglucanases can unproductively adsorb onto cellulose chain

[86]. Enzyme activity can also be lost due to thermal denaturation and shear force from mechanical mixing [87]. Impedances to enzymatic hydrolysis are illustrated in Figure 6.

Additives such as surfactants (Tween 20), bovine serum albumin, and polymers (PEG6000) increase enzymatic hydrolysis yields by binding to lignin instead of enzymes [88]. Eriksson et al. [89] found that enzyme adsorption to the substrate reduced from 90 to 80% upon addition of surfactant. Both glucose and xylose yields increase. The effectiveness of the additives depends on the type of pretreatment. Increase in sugar release was insignificant beyond additive loading of 150 mg/g glucan [88].

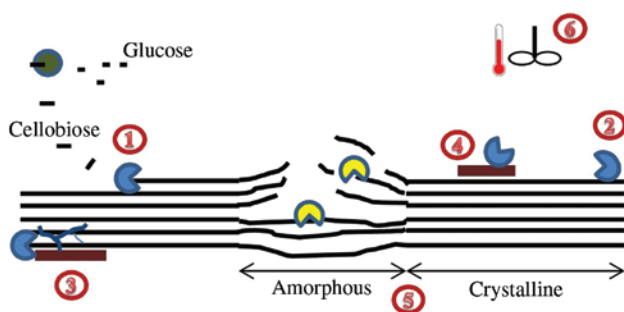


Figure 6: Factors affecting enzymatic hydrolysis of cellulose: (1) end-product inhibition by glucose and cellobiose; (2) unproductive binding of enzyme onto cellulose; (3) structural hindrance by lignin and hemicellulose; (4) unproductive binding of enzyme onto lignin; (5) cellulose crystallinity; and (6) shear- and thermal-induced denaturation.

4.2 Enzyme recycling

Recycling enzymes can offer potential enzyme cost savings. Recycling 60% of cellulose can generate cost savings of 15%, while 90% recycling results in savings of 50% [90]. Exo- and endo-glucanases remain adsorbed to the solid substrate during enzymatic hydrolysis. These enzymes can thus be recycled by recycling insoluble biomass fraction, which could result in 30% decrease in enzyme dosage [91]. Other ways of recycling enzymes

are recycling enzymes present in the complete reaction mixture and recycling enzymes present in the complete reaction mixture after all cellulose has been hydrolyzed [92]. The first one can be accomplished by a fed-batch process. For delignified biomass, the enzymes desorb from the solid substrate which results in recovery of all cellulose activity [91, 92]. Membrane filtration is another method of recycling enzymes [93–95]. Some 50-kDa polyethersulfone membranes can be used in the process [94]. Cost benefit of enzyme recycling with membranes can be as high as 18 cents/gal of ethanol produced [95]. The main concepts of recycling enzymes are shown in Figure 7.

4.3 Yield calculations

At low solids concentrations (<10%, w/w) glucose yields are calculated by the following equation:

$$Y_g = \frac{C_g - C_{g0}}{\varphi_G C_{is0} x_{G0}} \quad (1)$$

If soluble sugar oligomers are present in the pretreated slurry, they also need to be incorporated into the yield calculations:

$$Y_g = \frac{C_g - C_{g0}}{\varphi_G C_{is0} x_{G0} + \varphi_{gos} C_{gos0}} \quad (2)$$

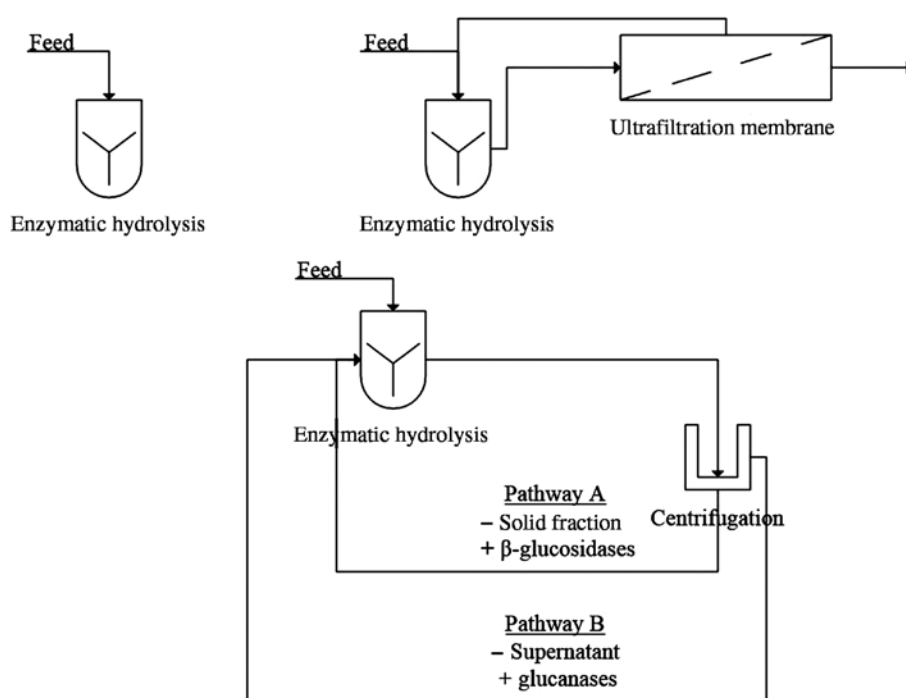


Figure 7: Various ways of recycling enzymes.

Equations (1) and (2) are subject to these assumptions [96]:

1. The density of the hydrolysis slurry is 1000 g/l.
2. The volume of the liquid equals that of the hydrolysis slurry.
3. The volume of the liquid remains unchanged during the hydrolysis.

However, for slurries that contain little or no free water (10%–40% solids content, w/w), enzymatic hydrolysis involves changes of volume, density, and proportion of insoluble solids [97]. At these concentrations, Eqs. (1) and (2) can overpredict glucose yields by as much as 30% (increasing with solids loading). The following equation was developed by Zhu et al. [96] to account for change of liquid volume and soluble components other than HPLC-detectable sugars:

$$Y_g = \frac{\left[C_g \left(\frac{V_h}{V_{h0}} \right) - C_{g0} \right] \left(\frac{1}{f_{ts0} x_{is0}} - 1 \right)}{\varphi_g \rho_{h0} x_{g0} + \varphi_{gos} C_{gos0} \left(\frac{1}{f_{ts0} x_{is0}} - 1 \right)} \quad (3)$$

The ratio of liquid volumes before and after enzymatic hydrolysis, $\frac{V_h}{V_{h0}}$, is calculated by

$$\frac{V_h}{V_{h0}} = \frac{\rho_{h0,c} - \sum (1 - \alpha_i) C_{i0}}{\rho_{h,c} - \sum (1 - \alpha_i) C_i} \quad (4)$$

where $\alpha_{cellobiose} = 0.05$, $\alpha_{glucose} = \alpha_{galactose} = \alpha_{mannose} = 0.01$, and $\alpha_{xylose} = \alpha_{arabinose} = 0.12$ are the correction factors to account for the amount of water consumed during the hydrolysis of respective sugar components. The liquid density is estimated by the following:

$$\rho_h = \rho_w + 0.35 \sum C_i \quad (5)$$

Using equations (3)–(5) gives good predictions of enzymatic hydrolysis yields with a relative error of 1%–5%. The error is slightly reduced if initial density of liquid is measured rather than calculated.

Roche et al. [98] proposed an equation that predicts the total biomass conversion in which conversion of both cellulose and hemicellulose are accounted for:

$$= \frac{r_{Gg} \Delta f_g + r_{Gcb} \Delta f_{cb} + r_{Xx} \Delta f_x}{f_{is0} (x_{g0} + x_{x0})} \quad (6)$$

In equation (6), sugar concentrations in the liquid are converted to mass fractions.

4.4 Future prospects

High cost of enzyme is one of the impediments to commercialization of lignocellulosic ethanol. More efficient enzyme cocktails would have to be created that offer improved catalytic activity and synergy. Strategies to improve enzymes include bioprocessing for superior key enzymes, mining plant pathogens for hydrolytic enzymes, and enzyme engineering of which the latter is of the most importance. It includes mutagenesis, DNA screening, and gene expression or overexpression [99, 100]. Conventional cellulose enzymes operate at a temperature of around 50°C. Thermostable enzymes have been developed that can function at a temperature range of 60–100°C. Operating at increased temperature would mean higher specific activity of enzymes, which would reduce enzyme loading and higher stability which would allow for longer hydrolysis times [101].

5 Fermentation

Saccharomyces cerevisiae is the most common yeast used in ethanol fermentation. For the purpose of fermenting sugars from lignocellulosics where ethanol concentration in the fermentation broth can only reach as high as 10% (w/w), yeast can be considered ethanol tolerant as growth is suppressed at 12% (w/v) ethanol but fermentative capacity is as high as 30% (w/v) ethanol. Protoplast fusion, hybridization, and continuous culture selection have been used to obtain ethanol-tolerant yeasts [102].

Saccharomyces cerevisiae yeast has been the main focus of researchers on improving its xylose fermenting ability. *S. cerevisiae* strains have been adapted to xylose metabolism by selection pressure, switching from cultivating on xylose to glucose-xylose and then back to xylose, and growing recombinant strains in aerobic environment and gradually moving to anaerobic environment [103]. Narrowed metabolic pathway of xylose conversion to ethanol is shown in Figure 8.

5.1 Simultaneous saccharification and fermentation

SSF gives higher ethanol yields and lower enzyme loading, which is required because fermenting microorganisms relieve end-product inhibition of enzymes. While the optimum pH of both enzymatic hydrolysis and fermentation is at 4.5, fermentation takes place at a lower optimum

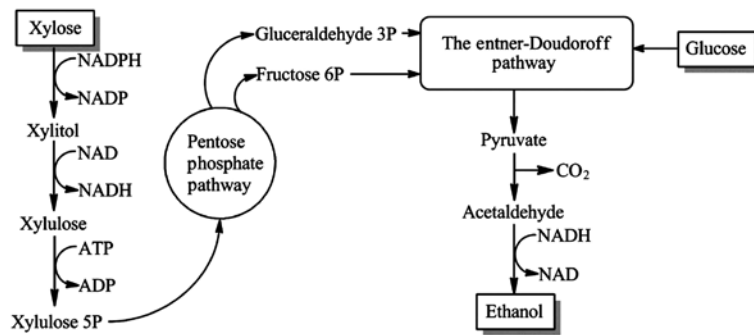


Figure 8: Xylose metabolism pathway in yeast (adapted from [104]).

temperature of 37°C [105]. To alleviate this problem and increase the temperature of SSF closer to the optimum of enzymes, Ballesteros et al. [106] has used thermo-tolerant yeasts capable of fermenting glucose at 42°C. Shaw et al. [107] engineered thermophilic bacteria strain capable of fermenting ethanol at 50°C. The strain required 2.5 times reduced enzyme loading for SSF compared to *S. cerevisiae* at 37°C. Factors affecting solid state fermentation include enzyme loading, biomass particle size, and mechanical shear produced by the impeller. Selected studies utilizing various strains for SSF are shown in Table 5.

5.2 Future developments

Using metabolic engineering to develop ethanol fermenting thermophiles that can function at a temperature above 50°C could be a new trend in lignocellulosic ethanol fermentation. Together with thermostable enzymes, SSF would take place at a much higher temperature than the conventional optimum of 37°C. This would result in even lower enzyme loading required and reduced fermentation times as sugars would be released from pretreated biomass at a much higher rate. These trends in metabolic

engineering of ethanol-fermenting bacteria could set a milestone in lignocellulosic ethanol production in the future and significantly reduce the economic barrier to its commercialization. Putting all the steps of the process together, one can picture an ionic-liquid-based biorefinery shown in Figure 9. This biorefinery would utilize cellulose and hemicellulose sugars to produce ethanol, and lignin would be used as a separate product to satisfy various needs.

6 Rheology of lignocellulosic biomass

Studies on rheology of lignocellulosic biomass for production of biofuels are mainly limited to dilute acid pretreated corn stover and spruce investigated over biomass concentration range of 4%–40% (w/w). It was shown that untreated/pretreated biomass slurries are shear-thinning fluids with considerable yield stress [112–115]. The non-Newtonian behavior begins at biomass concentrations above 5% (w/w) [112]. At biomass concentration ~20% (w/w) pretreated corn stover is a thick paste that can

Table 5: Ethanol yields in various simultaneous saccharification and fermentation of biomass utilizing various strains.

Strain	Solids (% wt.)	Temperature (°C)	Ethanol concentration (g/l)	Ethanol yield (%)	References
<i>Kluyveromyces marxianus</i> CECT 10875	10	42	19	72	[106]
<i>Saccharomyces cerevisiae</i>	n.a.	38	10.2	61	[108]
<i>Mucor indicus</i>	n.a.	38	11.4	68	[108]
<i>Rhizopus oryzae</i>	n.a.	38	12.4	74	[108]
<i>Escherichia coli</i> (KO11)	10	38	24.1	89	[109]
<i>Saccharomyces cerevisiae</i> D5A	10	38	12.7	83	[110]
<i>Saccharomyces cerevisiae</i>	10	40	23.7	53	[111]

n.a., not available.

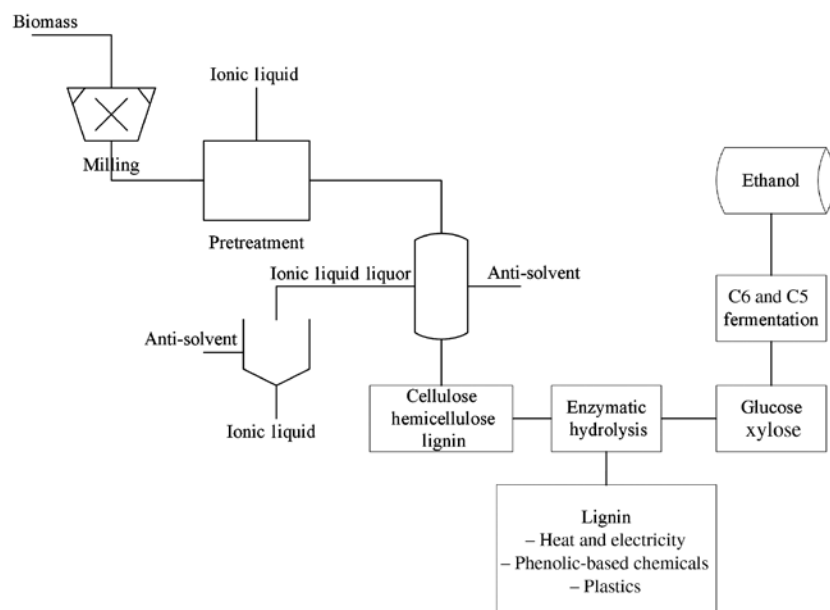


Figure 9: Ionic-liquid-based biorefinery.

undergo irreversible plastic deformation [113]. Yield stress and viscosity increase with increasing biomass concentration due to increased interaction between biomass fibers and particles [116]. These interactions become stronger as slurry concentration is increased due to mopping up of free water by biomass particles, which have high water-absorbing capacity. For instance, at concentration of 20% (w/w), the volume fraction of dilute acid pretreated corn stover is approximately 40% [98]. Contrary to other studies, Viamajala et al. [117] found that yield stress and viscosity reached a maximum point beginning from biomass concentration of 20% (w/w) depending on particle size and pre-treatment. At that point, the slurry was observed to be a wet granular material with little or no free water.

Yield stress is the most important rheological parameter of biomass slurries as it provides minimum requirements for transport and mixing equipment. The common power law relationship used to model yield stress as a function of insoluble solids concentration is

$$\tau_y = aC_m^b \quad (7)$$

The indexes depend on measurement technique employed and biomass properties such as particle size distribution and pretreatment [118]. Power law parameters for various biomass slurries are shown in Table 6. The power law index is in the range of 3.0–7.8. According to data published by Ehrhardt et al. [119], power law index decreased from 4.4 to 3.7 as pretreatment severity was increased. An opposite trend can be observed from

data published by Viamajala et al. [117], where pretreated samples had higher power law indices than untreated samples. Wiman et al. [115] found that decreasing particle size by milling increased power law index to 7.1 from 5.0. Similar results were reported by Viamajala et al. [117] where the power law index was increased from 3.0 to 4.0 as the particle size was reduced from 20 to 80 mesh. For wood pulp fibers, the power law index is reported in the narrower range of 2.3–3.6 [118]. This narrower range could be attributed to a more uniform size distribution of pulp fibers, while biomass such as corn stover was found to consist of particles and fibers with sizes ranging between microns and millimeters and aspect ratios ranging from 1 to 20 [113, 114].

Particle size and pretreatment severity are factors that directly affect rheological properties of lignocellulosic slurries. Larger particles will have larger fibers on its surface resulting in greater entanglement and particulate interactions and thus higher resistance to flow [116]. The yield stress of dilute acid pretreated spruce slurry (12%, w/w) decreased from 22.6 Pa to 0.55 Pa after milling [115]. Viamajala et al. [117] found that apparent viscosity of 15% (w/w) untreated corn stover decreased from ~200 Pa·s to ~100 Pa·s as particle size was reduced from 20 to 80 mesh, with the gap in viscosity between the two particle sizes increasing with increasing pretreatment severity. The yield stress also halved for untreated samples and was reduced by about 97% for pretreated samples (Table 5). Dasari and Berson [116] found that viscosity of 10% (w/w) oak sawdust slurries decreased from 3000 cP for particle

Table 6: Power law parameters for yield stress of biomass slurries.

Biomass	Range studied	Pretreatment/size	Conditions	a (10^6 Pa)	b	$\tau_{y(0.15)}$ (Pa)	References
Corn stover	5–30 wt%	Dilute acid/Lavg = 100 μ m	5% H_2SO_4 , 190 °C	9.6	5.7	193	[113]
Corn stover	5–17 wt%	Dilute acid/Lavg = 120 μ m	1.4% H_2SO_4	0.003	4.1	1.3	[112]
Corn stover	5–17 wt%	Dilute acid/500 μ m sieve	N/A	77	6.0	877	[114]
Corn stover	20–35 wt%	Dilute acid/300 μ m > Lavg < several cm	1.0% H_2SO_4 , 159°C	5.5	4.3	1576	[119]
			1.0% H_2SO_4 , 181°C	2.3	4.4	545	
			1.0% H_2SO_4 , 189°C	0.87	4.2	301	
			1.0% H_2SO_4 , 194°C	0.17	3.7	152	
			0.5% H_2SO_4 , 182°C	1.4	3.3	2674	
Corn stover	10–40 wt%	Untreated/80 mesh	Soaked in 1.5% H_2SO_4	0.42	4.0	221	[117]
		Dilute acid/80 mesh	1.5% H_2SO_4 , 190°C, 2 min	25	7.8	9.4	
		Untreated/20 mesh	Soaked in 1.5% H_2SO_4	0.14	3.0	473	
		Dilute acid/20 mesh	1.5% H_2SO_4 , 190 °C, 2 min	0.48	3.9	294	
Spruce	4–12 wt%	Dilute acid/2–10 mm	2.5% SO_2 , 210°C, 5 min	0.91	5.0	69	[115]
		Dilute acid/2–10 mm	2.5% SO_2 , 210°C, 5 min, then milled	1.9	7.1	2.7	

size range of $150 \mu\text{m} < x \leq 180 \mu\text{m}$ to 61.4 cP for particle size range of $33 \mu\text{m} < x \leq 75 \mu\text{m}$. Acidic pretreatment removes hydrophilic xylan polymer, which increases free water in the slurry and reduces particle size [117, 119]. Ehrhardt et al. [119] found that increasing either pretreatment temperature or acid concentration resulted in decrease in yield stress and plastic viscosity of dilute acid pretreated slurries. When reaction temperature was increased from 159°C to 194°C, the yield stress decreased by 95%. Similar results were obtained by Viamajala et al. [117]. Although stronger pretreatment and reduction in particle size can lead to significant reductions in both slurry viscosity and yield stress, the economic benefits of reduced power consumption during mixing due to improved flow properties need to outweigh the additional costs associated with those energy-intensive operations. It is not envisioned that their intensity would go beyond that required for efficient digestibility of cellulose by the enzymes.

During enzymatic hydrolysis, the slurry viscosity is rapidly reduced as hydrophilic cellulose microfibrils are broken down into sugars, resulting in reduction in particle size and increase in free water of the slurry. Dasari and Berson [116] found that viscosity of sawdust slurry was reduced by 70% of its initial value within the first 8 h of hydrolysis. The biggest drop occurred during the first 3.5 h of reaction. Similar pattern was obtained by Rosgaard et al. [120] for steam pretreated barley straw where the final viscosity after 72 h of hydrolysis reached below 100 mPa·s for all samples. The rate of viscosity decrease was slower for experiments with higher biomass loading.

Use of surfactants, such as sodium dodecylbenzene sulfonate, cetylpyridinium chloride, and cytel trimethyl ammonium bromide at concentration of 0.1% (w/w) can

result in 3–4-fold reduction in the yield stress and viscosity. The use of these additives can result in 0.7% reduction in total capital costs and 1.8% reduction in total electricity consumption [121]. Samaniuk et al. [122] studied water-soluble polymers (WSPs), surfactants, and fine particles as rheology modifiers. WSPs were most effective, resulting in 60%–80% reduction in yield stress at additive concentrations of 1%–2% (w/w dry biomass).

When dealing with suspension slurries such as biomass, precise rheological measurements may become difficult due to settling in the measurement devices and wall slip [113, 123]. Pimenova and Hanley [123] used a helical ribbon impeller to measure the rheology of dilute acid pretreated corn stover at concentrations of up to 30% (w/w) solids. The helical impeller was found to be ineffective at solids concentrations above 32% (w/w). The apparatus was calibrated using standard xanthan and guar gum solutions. In an interlaboratory study by Stickel et al. [113], rheology of dilute acid pretreated corn stover was measured by different rheometers (a wide-gap vane with parallel plates, a narrow-gap vane, roughened parallel plates with 100-grit sandpaper, and cone and plate geometries) for solid concentrations of up to 30% (w/w). To avoid settling, samples were well-mixed by hand prior to taking measurements. For parallel plates, large particles were screened out to prevent jamming. For the exception of cone and plate rheometer, there was a good agreement between the results of different laboratory groups. Roughened parallel plates were found to be able to cover all rheological properties studied.

Various models were used to represent stress-strain behavior of biomass slurries. These include power law, Bingham, Casson, and Herschel-Bulkley models. These models, however, are not applicable to enzymatic

hydrolysis, the process step where rheology plays a key role, because of rapid changes to biomass structure during the initial stages. Roche et al. [98] modelled yield stress of dilute acid pretreated corn stover during enzymatic hydrolysis at 20% (w/w) solid loading as a function of conversion and particle volume fraction. The model showed good agreement with experimental data, and work is underway to model viscosity in a similar manner. Such models that are based on physical principles could aid in reactor design and eliminate the need for conventional rheometric measurement techniques.

Rheological data on lignocellulosic biomass is limited to acidic pretreatments, and no information is available on rheology of biomass pretreated with other methods such as alkali or fractionative pretreatments. Acidic pretreatments remove hemicellulose, while alkali pretreatments target lignin, thus resulting in two fundamentally different substrates with different properties such as water absorbing capacity, which has a direct effect on slurry rheology. In the case of an alkali pretreatment, it is expected that rheological properties would be higher due to the presence of amorphous hemicellulose and swelling of biomass, which would result in much greater water absorbing capacity, limiting to a greater extent the available free water in the slurry and particulate mobility compared to pretreatment with an acid. There is also limited rheological data on different feedstock types such as woody biomass that contains more lignin. Higher lignin content could influence forces of attraction between fibers and thus affect rheology of the material [124].

7 Effect of hydrodynamics of mixing on biomass hydrolysis

Mixing enhances the hydrolysis of cellulose by improving the adsorption of the enzymes. For the cellulose enzyme complex, agitation has a direct effect on the adsorption of exoglucanase, while the adsorption of endoglucanase is not greatly affected. As a result of this shift in adsorption balance of cellulose enzymes, synergistic effect takes place that favors enzymatic hydrolysis [125]. Figure 10 shows the effect of mixing on enzymatic hydrolysis of biomass as obtained using various systems that were utilized in different previous works. As can be seen in Figure 10, enzymatic hydrolysis yields increase for all biomass concentrations as a more effective mixing method is applied. A study by Roche et al. [126] using roller bottle bioreactor shows that mixing effectiveness is more pronounced as solid concentration is increased. However, Dasari [127] found that improvement in enzymatic hydrolysis yield during mixing with scraped surface bioreactor (SSBR) was uniform with solids concentration. Mixing in shake flasks at high solids content is not as effective as mixing in roller bottles, and the latter should be used in studies at high solids content to eliminate mass transfer limitations from parameters studied.

There is also a synergistic effect between agitation and enzymatic hydrolysis. Mixing increases the rate of enzymatic hydrolysis, while cellulose hydrolysis reduces slurry viscosity and enhances mixing. Torque profile mixing is shown in Figure 11. Initially, torque is high to overcome

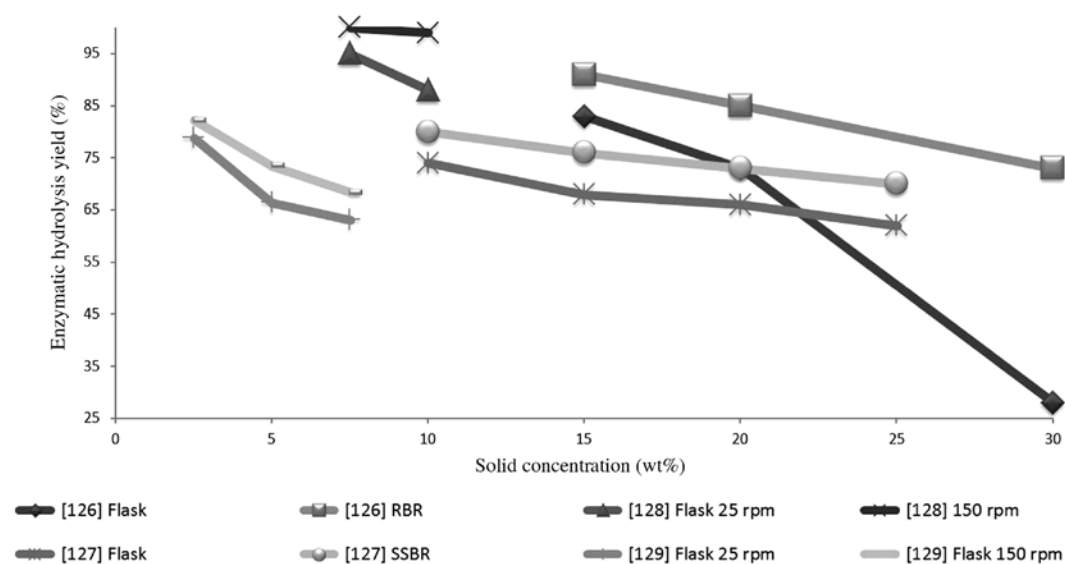


Figure 10: Effect of mixing on enzymatic hydrolysis.

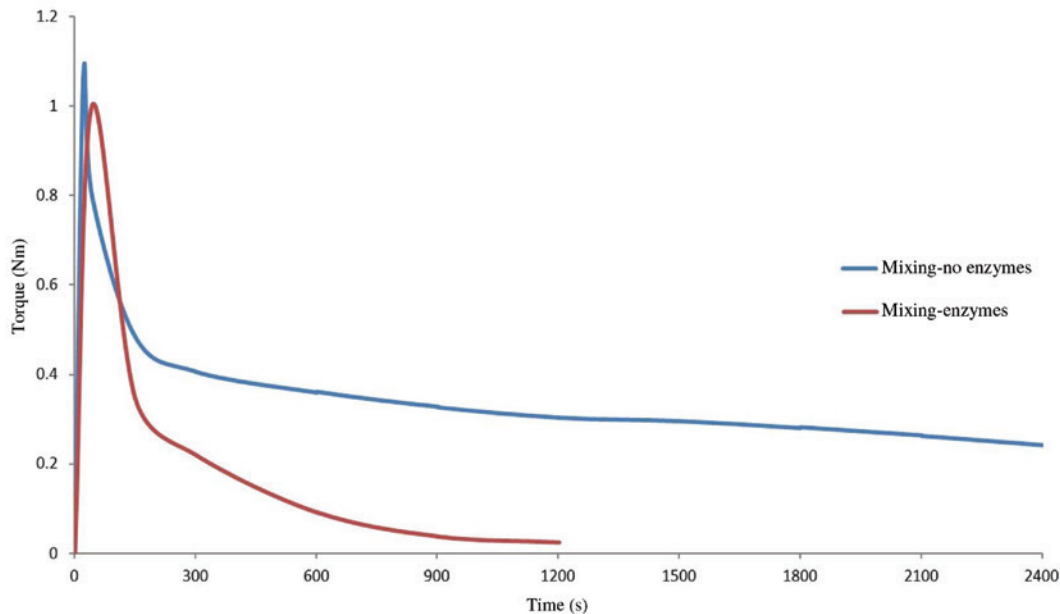


Figure 11: Torque for mixing of dilute acid pretreated corn stover (20%, w/w solids) (data obtained from [130]).

the yield stress, and it reduces over time as biomass particles are set in motion. The case of mixing without enzymes displays this shear-thinning behavior of biomass. When the enzymes are added, there is a steep decline in torque over time. Samaniuk et al. [130] studied the mechanism of mixing during enzymatic hydrolysis of biomass slurries at solids loading of 20% (w/w). Mixing was carried out in a modified torque rheometer with counter-rotating screw elements. Mixing speed was 55 rpm, and enzyme loading was 10 filter paper unit (FPU)/g cellulose. Samples mixed without enzymes showed a decrease in fiber length over the first 600s. When enzymes were added, there was a greater decrease in fiber length over time. It was hypothesized that the synergy between mixing and enzymatic hydrolysis was due to particle size reduction and damage of fibers by enzymes would leave them more susceptible to breakage by shear force. Palmqvist et al. [131] found that mechanical “pre-shearing” of substrate before adding enzymes had no significant effect on enzymatic hydrolysis. Lenting and Warmoeskerken [132] hypothesized that mechanical shear breaks crystalline cellulose regions into amorphous state, making them more amenable to saccharification by enzymes.

Enzyme dosage has a large effect on mixing energy consumption at increased solids loading. Zhang et al. [11] found that the ratio of mixing energy consumption to thermal energy in the ethanol produced increased exponentially from 9.3% at solids loading of 15% (w/w) to 58.6% at solids loading of 30% (w/w) at enzyme dosage of 7 FPU/g DM (dry matter) in an energy-efficient

helical stirring bioreactor. When the enzyme dosage was increased to 30 FPU/g DM at solids loading of 30% (w/w), the ratio decreased to 12.7%. The cost of enzymes would have to be substantially reduced to account for increased enzyme dosage required for energy-efficient mixing of biomass at high solids content.

7.1 Stirred tanks

Power consumption is the most important parameter in mixing. Achieving high degree of homogeneity at low power consumption is the objective of any mixing process. Power consumed is calculated by the following equation:

$$P = P_0 \rho N^3 D^5 \quad (8)$$

Power number is a function of impeller Reynolds number in laminar region:

$$Re_i = \frac{\rho N D^2}{\mu} \quad (9)$$

In turbulent region ($Re_i > 10^4$), power number depends on impeller and reactor design parameters [131]. These parameters include ratio of reactor diameter to height, ratio of impeller tip diameter to reactor diameter, and the presence of baffles [133]. Design value allocated for mixing power consumption during SSF at National Renewal Energy Laboratory (NREL) pilot plant facility and utilized dilute-acid pretreated corn stover is 60 W/m³. The process is operated

at solids content of 10% (w/w) [134]. Stirred tanks are also used in enzymatic hydrolysis at Iogen's pilot plant in Canada. Plant capacity is 40 t/day, and solids loadings were between 15 and 20% (w/w) [5]. No information is given on the type of impellers used in these processes.

Palmqvist et al. [131] studied conversion and mixing power consumption of steam-pretreated spruce in a stirred tank at solids loading of 10% (w/w). The reactor was equipped with a pitched-blade impeller pumping upwards. Experiments were conducted at enzyme loadings of 10 and 20 FPU/g glucan and at impeller speeds between 25 and 500 rpm. At 500 rpm the conversion was double that at 25 rpm. Linear relationship was established between impeller speed and conversion at both enzyme loadings. The following relationship was found for the power number:

$$P_o = \frac{346.7}{Re_i} + 1.27 \quad (10)$$

Extremely high power requirement, 1.5 kW/m³, was reported for maximum conversion of 72% after 96 h. An optimum power requirement of 50 W/m³ required operating at impeller speeds between 25 and 75 rpm at which the conversions were too low. Doubling enzyme loading reduced energy consumption by 15 to 25% depending on mixing speed.

The type of feedstock used during enzymatic hydrolysis affects power requirements for the process. Palmqvist and Lidén [124] studied power input during enzymatic hydrolysis of steam-pretreated energy crop *Arundo donax* (giant reed) and spruce in a stirred tank equipped with an anchor impeller at solids loading up to 20% (w/w). The experiment was conducted at either constant impeller speed or the impeller power input. At fixed impeller speed of 10 rpm, glucose yields increased for spruce but decreased for arundo with increasing solids content. Total energy input was much larger for spruce than arundo. Power input did not have a significant effect on enzymatic hydrolysis yields for arundo, but it did for spruce. It was concluded that process design for enzymatic hydrolysis reactor should be substrate specific as there were large differences in fiber structure and lignin content of the two materials, resulting in different rheological characteristics.

Hoyer et al. [135] studied SSF of steam exploded softwood in stirred tanks at solids loading of 5%–12% (w/w). Turbine impeller was used at impeller speed of 700 rpm, and an anchor impeller was used at speeds of 200 and 700 rpm. At solids loading of 10% (w/w) and impeller speed of 700 rpm, anchor impeller gave a slightly better ethanol yield compared to turbine impeller. At 12% (w/w),

solids loading turbine impeller was not investigated, and the ethanol yield for anchor impeller dropped dramatically from 95.8% at 10% (w/w) to 32.7% at 12% (w/w). At impeller speed of 200 rpm, ethanol yield for anchor impeller at solid loading of 10% (w/w) was reduced to 84.6%.

Stirred tanks have been used on a milliliter scale for screening studies for enzymatic hydrolysis. Riedlberger et al. [133] designed two stirrers, the H-stirrer consisting of two vertical blades situated parallel to each other along the shaft and the S-stirrer with one blade pointing downwards and the other one pointing upwards. The stirrers were magnetically driven by a magnet located in the middle of the impeller. The time to achieve homogeneity was twice as high for H-stirrer compared to S-stirrer. S-stirrer with baffles gave the best enzymatic hydrolysis yield. Enzymatic hydrolysis of corn stover was performed at solids loading of 6% (w/w). Computational fluid dynamics showed that the S-stirrer had a strong axial flow field, while for the H-stirrer, tangential flow dominated. In a previous study, the S-stirrer was capable of mixing microcrystalline cellulose at 20% (w/w) solids and wheat straw at 8%–10% (w/w) and was successfully scaled up to 1 l volume from 10 ml. The main purpose of the block of parallel stirred tank reactors was to provide an efficient tool for optimization of enzymatic hydrolysis parameters such as pretreatment conditions, enzyme dosages, and combinations [136].

Mixing of viscous fluids with yield stress in stirred tanks results in formation of a cavern where shear stress equals yield stress at the cavern boundary and unmixed regions result outside of the cavern boundary (see Figure 12). Solomon et al. [137] proposed a mathematical model for mixing cavern, assuming a spherical shape centered on the impeller. Hot film anemometry and Xanthan gum were used in the experiments. Power dissipated by the impeller is transmitted to the cavern wall, and it is assumed that tangential motion dominates within the cavern. Cavern diameter can be obtained by

$$\left(\frac{D_c}{D}\right)^3 = \left(\frac{4P_o}{\pi^3}\right) \left(\frac{N^2 D^2 \rho}{\tau_y}\right) \quad (11)$$

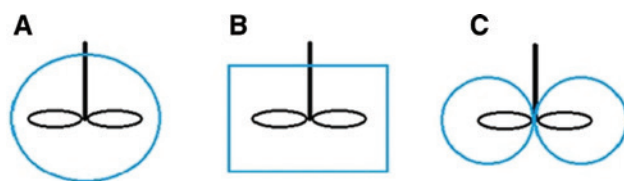


Figure 12: Various caverns: (A) spherical, (B) cylindrical, and (C) torus.

Spherical representation of the cavern model is not exact. It was found that the cavern is somewhat squashed. Elson et al. [138] modified the spherical model into cylindrical model:

$$\left(\frac{D_c}{D}\right)^3 = \frac{1}{\pi^2 \left(\frac{H_c}{D_c} + \frac{1}{3}\right)} P_{ot} \left(\frac{\rho N^2 D^2}{\tau_y}\right) \quad (12)$$

The value $\frac{H_c}{D_c} = 0.4$ is a good approximation until the cavern boundary reaches baffles. Amanullah et al. [139] has developed an equation for a torus-shaped model with cavern spheres touching at the center of the impeller:

$$\left(\frac{D_c}{D}\right)^2 = \frac{1}{\pi} \left(\frac{N^2 D^2 \rho}{\tau_y}\right) \sqrt{N_f^2 + \left(\frac{4P_o}{3\pi}\right)} \quad (13)$$

The model takes into account total momentum produced by the impeller as the summation of both tangential and axial components and can also be applied to radial flow impellers.

7.2 Helical bioreactor

Helical ribbon bioreactors provide the advantage of high mixing efficiency at low power consumption for stirring high solids loading lignocellulosic slurries. Zhang et al. [11] used a helical stirring bioreactor for SSF of steam exploded corn stover by *S. cerevisiae* DQ1 strain at solids loading of 15%–30% (w/w). The reactor consisted of a drive shaft, a helix impeller, a turbine/aerofoil impeller on the drive shaft in the middle of the helix impeller, and a bottom impeller. The SSF was operated in two stages. In the first stage, the prehydrolysis stage, biomass is liquefied into a liquid slurry form for 12 h. The biomass feeding rate is adjusted in a semicontinuous style so that solids are first liquefied prior to feeding any additional solids. In the SSF stage, the biomass slurry is fermented for 60 h. The feeding time in the prehydrolysis stage was 2 h shorter for the helical impeller than Rushton impeller showing that the helical impeller was more efficient at mixing biomass in the crucial initial stage of SSF operation. Quicker liquefaction would mean a shorter overall process time that would yield cost savings.

Compared to Rushton impeller, glucose consumption during SSF for helical impeller was greater even though glucose concentration was identical for both cases at the start of fermentation. Higher glucose consumption resulted in higher ethanol production and a greater final

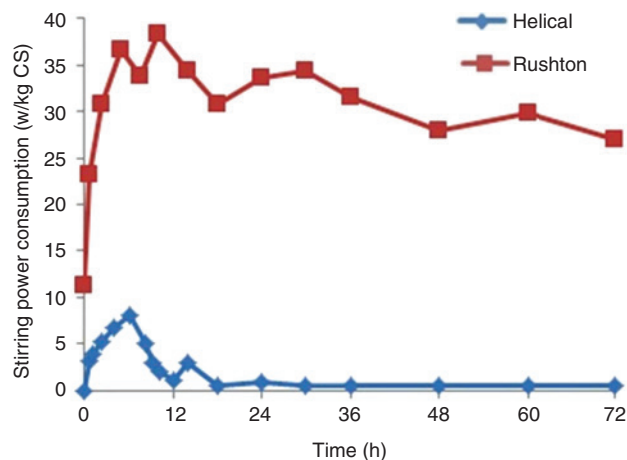


Figure 13: Comparison between mixing power consumption of helical vs. Rushton impellers during prehydrolysis (Rushton: 14 h; helical: 12 h) and SSF of steam exploded corn stover (CS) at solids loading of 30% (w/w) and enzyme dosage of 15 FPU/g DM (data obtained from [11]).

ethanol concentration. Mixing power consumption is shown in Figure 13.

Computational fluid dynamics simulation showed that in a highly viscous system, fluid field distribution for the helical impeller was quite complex. There was a large vertical circulation with an upward flow near the axis, a downward flow between the outer edge of the impeller and the reactor wall, and small circulation around the spiral bladders. For the Rushton impeller, the mixing field was limited to one third of the whole reactor volume around the blades, while the helical impeller showed a uniform distribution throughout the whole reactor volume [11].

7.3 Rotating drums

Drum mixers operate by the principle of gravity mixing where biomass is subjected to free fall by the rotating drum or axis containing lifting paddles. When compared to conventional stirred tanks, drum mixers enable efficient mixing of high dry matter content biomass slurries (up to 40%, w/w) at low energy expenditures. The rotating drums can be easily scaled up to fit various process needs or biomasses. Free fall mixer is currently in use at DONG Energy's Integrated Biomass Utilization System pilot plant facility for pre-hydrolysis and SSF operation [4]. Horizontal operation of drum mixers provides advantages such as eliminating particle settling and formation of dead zones as well as improved heat transfer through reactor wall [140].

Roche et al. [98] compared enzymatic hydrolysis performance of 2 l roller bottles to a custom designed high solids bioreactor (HSBR). The reactor included a 5 l cylinder with eight paddles and wiper blades mounted on a horizontal rotating shaft. The wiper blades were installed to clear the wall of the reactor to enable mixing at high solids content (20%, w/w). The mixing speed was 2 rpm. The HSBR gave a better enzymatic hydrolysis yield (about 5%) than roller bottle at enzyme loading of 20 mg protein/g cellulose. Roller bottles were also investigated for parameters such as mixing speed (2–20 rpm), presence of baffles (zero or four baffles), and amount of mixing media (0–18 media). Biomass conversion was not significantly affected by the aforementioned parameters.

Jørgensen et al. [141] studied a horizontal drum bioreactor with varying mixing speeds (3.3–11.5 rpm) and mixing media (3–12 kg of steam exploded wheat straw) at solids loading above 20% (w/w). The reactor was a horizontal drum divided into five chambers. Mixing was achieved by a horizontal shaft mounted with three paddlers. The motor was programmed to shift twice a minute between clockwise and anticlockwise rotation. There was no significant correlation between mixing speed and cellulose conversion as well as ethanol yield. Hemicellulose conversion was found to decrease by 18% as mixing speed was increased from 3.3 to 11.5 rpm. At chamber filling of 3 kg, issues with adhesion of substrate to reactor walls and paddlers occurred, which resulted in the lowest cellulose conversion and ethanol yield. Above 4 kg, no major effect of chamber filling was revealed.

Dasari et al. [140] tested a novel SSBR for power consumption during saccharification of dilute acid pretreated corn stover slurries at solids loading of 10%–25% (w/w). The 8 l SSBR consisted of three scraping blades spaced 120° apart, connected to a central shaft and staggered along the shaft in three segments. Styrene rubber strips were attached along the length of each blade to scrape the interior of the reactor wall. For the highest solids content slurry tested (25%, w/w), the specific power consumption at mixing speed of 2 rpm was 0.56 kW/m³, which is below the lower limit of 1–5 kW/m³ power consumption for industrial applications. Glucose conversion at this mixing speed reached 70%.

8 Conclusion

A variety of pretreatments exist for conversion of lignocellulosics into ethanol. As not all of them are economically viable, an in-depth economic analysis would have to be

applied to screen for the best pretreatment options. New initiatives would also have to be undertaken to find more efficient ways of fracturing biomass. If it comes to the structural characteristics of biomass, genetically modified crops low in lignin would have to be grown globally. High-throughput screening techniques need to be developed to aid the search for better enzyme mixtures or ethanol fermenting microorganisms. More rheological data need to be obtained for a more open picture on determining the best pretreatment for rheological properties. Appropriate models will have to be constructed and compared as to which model represents the best fit to the experimental data. Novel mixing systems would have to be designed. Lignocellulosic ethanol research and development has reached a turning point where small improvements in each step of the process would have to be made to turn the tide towards large-scale commercialization.

Nomenclature

Y_g	Glucose yield
a_i	Amount of water used to form soluble sugar i from its polysaccharide (g/g of sugar i)
C_g	Concentration of glucose (g/l)
C_{g0}	Initial concentration of glucose (g/l)
C_{gos0}	Initial concentration of glucose oligomers (g/l)
C_i	Concentration of sugar i (g/l)
C_{i0}	Initial concentration of sugar i (g/l)
C_{is0}	Initial concentration of insoluble solids (g/l)
ρ_h	Density of hydrolyzate liquid at 25°C (g/l)
$\rho_{h,c}$	Calculated density of hydrolyzate liquid at 25°C (g/l)
$\rho_{ho,c}$	Calculated initial density of hydrolyzate liquid at 25°C (g/l)
ρ_w	Density of water at 25°C (g/l)
φ_G	Molecular weight ratio of glucose to glucan monomer (180/162)
φ_{gos}	Molecular weight ratio of glucose to average monomer weight of glucose oligomers (180/166.5, assuming oligomer DP of 4)
f_{iso}	Initial mass fraction of total solids (soluble + insoluble) in slurry total biomass conversion
f_{is0}	Initial mass fraction of insoluble solids in slurry
f_g	Glucose mass fraction of the total slurry
f_{cb}	Cellobiose mass fraction of the total slurry
f_x	Xylose mass fraction of the total slurry
γ_{Gg}	Molecular weight ratio of glucan monomer to glucose (162/180)
γ_{Gcb}	Molecular weight ratio of two glucan monomers to cellobiose (324/342)
γ_{Xx}	Molecular weight ratio of xylan monomer to xylose (132/150)
χ_{is0}	Initial mass fraction of insoluble solids in total solids
χ_{G0}	Initial mass fraction of glucan in insoluble solids
χ_{x0}	Initial mass fraction of xylan in insoluble solids
τ_y	Yield stress (Pa)

a	Consistency index (Pa)
b	Power law index
C_m	Mass fraction of insoluble solids
P	Power consumption (W)
P_o	Power number
N	Impeller speed (rps)
D	Impeller diameter (m)
ρ	Fluid density (kg/m ³)
μ	Fluid viscosity (Pa·s)
R_{ei}	Impeller Reynolds number
D_c	Cavern diameter (m)
H_c	Cavern height (m)
P_{ot}	Power number in the turbulent region
N_f	Axial force number

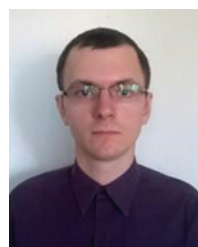
References

- [1] Viikari L, Vehmaanperä J, Koivula A. *Biomass Bioenergy* 2012, 46, 13–24.
- [2] Hahn-Hägerdal B, Galbe M, Gorwa-Grauslund MF, Lidén G, Zacchi G. *Trends Biotechnol.* 2006, 24, 549–556.
- [3] Schell DJ, Riley CJ, Dowe N, Farmer J, Ibsen KN, Ruth MF, Toon ST, Lumpkin RE. *Bioresour. Technol.* 2004, 91, 179–188.
- [4] Larsen J, Petersen MØ, Thirup L, Li HW, Iversen FK. *Chem. Eng. Technol.* 2008, 31, 765–772.
- [5] Tolan JS. *Clean Technol. Environ. Policy* 2002, 3, 339–345.
- [6] Volynets B, Dahman Y. *Int. J. Energy Environ.* 2011, 2, 427–446.
- [7] Sticklen M. *Curr. Opin. Biotechnol.* 2006, 17, 315–319.
- [8] Kim S, Dale BE. *Biomass Bioenergy* 2004, 26, 361–375.
- [9] Faraco V, Hadar Y. *Renew. Sustainable Energy Rev.* 2011, 15, 252–266.
- [10] Petersen MØ, Larsen J, Thomsen MH. *Biomass Bioenergy* 2009, 33, 834–840.
- [11] Zhang J, Chu D, Huang J, Yu Z, Dai G, Bao J. *Biotechnol. Bioeng.* 2010, 105, 718–728.
- [12] Li Q, Gao Y, Wang H, Li B, Liu C, Yu G, Mu X. *Bioresour. Technol.* 2012, 125, 193–199.
- [13] Saha BC, Yoshida T, Cotta MA, Sonomoto K. *Ind. Crop. Prod.* 2013, 44, 367–372.
- [14] Yang L, Cao J, Jin Y, Chang H, Jameel H, Phillips R, Li Z. *Biore-sour. Technol.* 2012, 124, 283–291.
- [15] Amiri H, Karimi K, Zilouei H. *Bioresour. Technol.* 2014, 152, 450–456.
- [16] Saha BC, Cotta MA. *New Biotechnol.* 2010, 27, 10–16.
- [17] Han M, Kang KE, Kim Y, Choi G-W. *Process Biochem.* 2013, 48, 488–495.
- [18] Benjamin Y, Cheng H, Görgens JF. *Ind. Crop. Prod.* 2013, 51, 7–18.
- [19] Sundar S, Bergey NS, Salamanca-Cardona L, Stipanovic A, Driscoll M. *Carbohydr. Polym.* 2014, 100, 195–201.
- [20] Kumar S, Kothari U, Kong L, Lee YY, Gupta RB. *Biomass Bioen-ergy* 2011, 35, 956–968.
- [21] Wang Z, Zhu JY, Zalesny Jr RS, Chen KF. *Fuel* 2012, 95, 606–614.
- [22] Santos RB, Treasure T, Gonzalez R, Phillips R, Lee JM, Jameel H, Chang H. *Bioresour. Technol.* 2012, 117, 193–200.
- [23] Sun Y, Cheng J. *Bioresour. Technol.* 2002, 83, 1–11.
- [24] Balat M. *Energy Convers. Manage.* 2011, 52, 858–875.
- [25] Gírio FM, Fonseca C, Carvalho F, Duarte LC, Marques S, Bogel-Lukasik R. *Bioresour. Technol.* 2010, 101, 4775–4800.
- [26] Buranov AU, Mazza G. *Ind. Crop. Prod.* 2008, 28, 237–259.
- [27] Vermerris W. In *Genetic Improvement of Bioenergy Crops*, 1st ed. Vermerris W, editor. Springer Science and Business Media: New York, 2008, Vol. 1, p 89.
- [28] Sathitsuksanoh N, Xu B, Zhao B, Zhang Y-HP. *PLoS One* 2013, 8, 1–6.
- [29] Fu C, Mielenz JR, Xiao X, Ge Y, Hamilton CY, Rodriguez M Jr, Chen F, Foston M, Ragauskas A, Bouton J, Dixon RA, Wang Z-Y. *Proc. Natl. Acad. Sci.* 2011, 108, 3803–3808.
- [30] Shen H, Poovaiah CR, Ziebell A, Tschaplinski TJ, Pattathil S, Gjersing E, Engle NL, Katahira R, Pu Y, Sykes R, Chen F, Ragauskas AJ, Mielenz JR, Hahn MG, Davis M, Stewart CN Jr, Dixon RA. *Biotechnol. Biofuels* 2013, 6, 71–86.
- [31] Himmel ME, Ding S-Y, Johnson DK, Adney WS, Nimlos MR, Brady JW, Foust TD. *Science* 2007, 315, 804–807.
- [32] Varga E, Réczey K, Zacchi G. *Appl. Biochem. Biotechnol.* 2004, 113–116, 509–523.
- [33] Heitz M, Capek-Ménard E, Koeberle PG, Gagné J, Chornet E, Overend RP, Taylor JD, Yu E. *Bioresour. Technol.* 1991, 35, 23–32.
- [34] Wu MM, Chang K, Gregg DJ, Boussaid A, Beatson RP, Saddler JN. *Appl. Biochem. Biotechnol.* 1999, 77–79, 47–54.
- [35] Avci A, Saha BC, Dien BS, Kennedy GJ, Cotta MA. *Bioresour. Technol.* 2013, 130, 603–612.
- [36] Zhu Y, Lee YY, Elander RT. *Appl. Biochem. Biotechnol.* 2005, 121–124, 1045–1054.
- [37] Kootstra AMJ, Beertink HH, Scott EL, Sanders JPM. *Biotechnol. Biofuels* 2009, 2, 31–45.
- [38] Mosier N, Hendrickson R, Ho N, Sedlak M, Ladisch MR. *Biore-sour. Technol.* 2005, 96, 1986–1993.
- [39] Wang Z, Cheng JJ. *Energy Fuels* 2011, 25, 1830–1836.
- [40] Kim S, Holtzaple MT. *Bioresour. Technol.* 2005, 96, 1994–2006.
- [41] Hu Z, Wen Z. *Biochem. Eng. J.* 2008, 38, 369–378.
- [42] McIntosh S, Vancov T. *Biomass Bioenergy* 2011, 35, 3094–3103.
- [43] Kang KE, Jeong G-T, Sunwoo C, Park D-H. *Bioprocess Biosyst. Eng.* 2012, 35, 77–84.
- [44] Teymouri F, Laureano-Perez L, Alizadeh H, Dale BE. *Bioresour. Technol.* 2005, 96, 2014–2018.
- [45] Varga E, Schmidt AS, Réczey K, Thomsen AB. *Appl. Biochem. Biotechnol.* 2003, 104, 37–50.
- [46] García-Cubero MT, González-Benito G, Indacoechea I, Coca M, Bolado S. *Bioresour. Technol.* 2009, 100, 1608–1613.
- [47] Banerjee G, Car S, Scott-Craig JS, Hodge DB, Walton JD. *Bio-technol. Biofuels* 2011, 4, 16–31.
- [48] Li C, Knierim B, Manisseri C, Arora R, Scheller HV, Auer M, Vogel KP, Simmons BA, Singh S. *Bioresour. Technol.* 2010, 101, 4900–4906.
- [49] Sathitsuksanoh N, Zhu Z, Zhang Y-HP. *Cellulose* 2012, 19, 1161–1172.
- [50] Park N, Kim H-Y, Koo B-W, Yeo H, Choi I-G. *Bioresour. Technol.* 2010, 101, 7046–7053.
- [51] Kim KH, Hong J. *Bioresour. Technol.* 2001, 77, 139–144.
- [52] Bitra VSP, Womac AR, Igathinathane C, Miu PI, Yang YT, Smith DR, Chevanan N, Sokhansanj S. *Bioresour. Technol.* 2009, 100, 6578–6585.

- [53] Bitra VSP, Womac AR, Chevanan N, Miu PI, Igathinathane C, Sokhansanj S, Smith DR. *Powder Technol.* 2009, 193, 32–45.
- [54] Sant'Ana da Silva A, Inoue H, Endo T, Yano S, Bon EPS. *Biore-sour. Technol.* 2010, 101, 7402–7409.
- [55] Yu Z, Zhang B, Yu F, Xu G, Song A. *Biore-sour. Technol.* 2012, 121, 335–341.
- [56] Rabelo SC, Filho RM, Costa AC. *Appl. Biochem. Biotechnol.* 2009, 153, 139–150.
- [57] Schmidt AS, Thomsen AB. *Biore-sour. Technol.* 1998, 64, 139–151.
- [58] Silverstein RA, Chen Y, Sharma-Shivappa RR, Boyette MD, Osborne J. *Biore-sour. Technol.* 2007, 98, 3000–3011.
- [59] Yamashita Y, Shono M, Sasaki C, Nakamura Y. *Carbohydr. Polym.* 2010, 79, 914–920.
- [60] Diaz A, Toullec JL, Blandino A, Ory I, Caro I. *Chem. Eng. Trans.* 2013, 32, 949–954.
- [61] Li Q, He Y-C, Xian M, Jun G, Xu X, Yang J-M, Li L-Z. *Biore-sour. Technol.* 2009, 100, 3570–3575.
- [62] Li B, Asikkala J, Filpponen I, Argyropoulos DS. *Ind. Eng. Chem. Res.* 2010, 49, 2477–2484.
- [63] Zhang Y-HP, Ding SY, Mielenz JR, Cui JB, Elander RT, Laser M, Himmel ME, McMillan JR, Lynd LR. *Biotechnol. Bioeng.* 2007, 97, 214–223.
- [64] Zhao X, Cheng K, Liu D. *Appl. Microbiol. Biotechnol.* 2009, 82, 815–827.
- [65] Sannigrahi P, Miller SJ, Ragauskas AJ. *Carbohydr. Res.* 2010, 345, 965–970.
- [66] Araque E, Parra C, Freer J, Contreras D, Rodríguez J, Mendonca R, Baeza J. *Enzyme Microb. Tech.* 2008, 43, 214–219.
- [67] Gu T. In *Green Biomass Pretreatment for Biofuels Production*, Gu T, editor. Springer: Netherlands, 2013, Vol. 1, p 107.
- [68] Narayanaswamy N, Faik A, Goetz DJ, Gu T. *Biore-sour. Technol.* 2011, 102, 6995–7000.
- [69] Bak JS, Ko JK, Choi I-G, Park Y-C, Seo J-H, Kim KH. *Biotechnol. Bioeng.* 2009, 104, 471–482.
- [70] Malherbe S, Cloete TE. *Rev. Environ. Sci. Bio.* 2002, 1, 105–114.
- [71] Keller FA, Hamilton JE, Nguyen QA. *Appl. Biochem. Biotechnol.* 2003, 105–108, 27–41.
- [72] Tao L, Aden A, Elander RT, Pallapolu VR, Lee YY, Garlock RJ, Balan V, Dale BE, Kim Y, Mosier NS, Ladisch MR, Falls M, Holtzapapple MT, Sierra R, Shi J, Ebrik MA, Redmond T, Yang B, Wyman CE, Hames B, Thomas S, Warner RE. *Biore-sour. Technol.* 2011, 102, 11105–11114.
- [73] Kazi FK, Fortman JA, Anex RP, Hsu DD, Aden A, Dutta A, Kothandaraman G. *Fuel* 2010, 89, S20–S28.
- [74] Eggeman T, Elander RT. *Biore-sour. Technol.* 2005, 96, 2019–2025.
- [75] Teeri TT. *Trends Biotechnol.* 1997, 15, 160–167.
- [76] Dashtan M, Schraft H, Qin W. *Int. J. Biol. Sci.* 2009, 5, 578–595.
- [77] Kuhad RC, Gupta R, Singh A. *Enzyme Res.* 2011, 2011, 1–10.
- [78] Shallom D, Shoham Y. *Curr. Opin. Microbiol.* 2003, 6, 219–228.
- [79] Våljamäe P, Kipper K, Pettersson G, Johansson G. *Biotechnol. Bioeng.* 2003, 84, 254–257.
- [80] Zhang M, Su R, Qi W, He Z. *Appl. Biochem. Biotechnol.* 2010, 160, 1407–1414.
- [81] Selig MJ, Knoshaug EP, Adney WS, Himmel ME, Decker SR. *Biore-sour. Technol.* 2008, 99, 4997–5005.
- [82] Ye L, Su X, Schmitz GE, Moon YH, Zhang J, Mackie RI, Cann IKO. *Appl. Environ. Microbiol.* 2012, 78, 7048–7059.
- [83] Zhu L, O'Dwyer JP, Chang VS, Granda CB, Holtzapapple MT. *Biore-sour. Technol.* 2008, 99, 3817–3828.
- [84] Chang VS, Holtzapapple MT. *Appl. Biochem. Biotechnol.* 2000, 84–86, 5–37.
- [85] O'Dwyer JP, Zhu L, Granda CB, Holtzapapple MT. *Biore-sour. Tech-nol.* 2007, 98, 2969–2977.
- [86] Zhang Y-H, Lynd LR. *Biotechnol. Bioeng.* 2004, 88, 797–824.
- [87] Ye Z, Hatfield KM, Berson RE. *Biore-sour. Technol.* 2012, 106, 133–137.
- [88] Kumar R, Wyman CE. *Biotechnol. Bioeng.* 2009, 102, 1544–1557.
- [89] Eriksson T, Börjesson J, Tjerneld F. *Enzyme Microb. Tech.* 2002, 31, 353–364.
- [90] Steele B, Raj S, Nghiem J, Stowers M. *Appl. Biochem. Biotech-nol.* 2005, 121–124, 901–910.
- [91] Weiss N, Börjesson J, Pedersen LS, Meyer AS. *Biotechnol. Biofuels* 2013, 6, 5–19.
- [92] Lee D, Yu AHC, Saddlert JN. *Biotechnol. Bioeng.* 1995, 45, 328–336.
- [93] Hong J, Tsao GT, Wankat PC. *Biotechnol. Bioeng.* 1981, 23, 1501–1516.
- [94] Knutsen JS, Davis RH. *Appl. Biochem. Biotechnol.* 2004, 113–116, 585–599.
- [95] Mores WD, Knutsen JS, Davis RH. *Appl. Biochem. Biotechnol.* 2001, 91–93, 297–309.
- [96] Zhu Y, Malten M, Torry-Smith M, McMillan JD, Stickel JJ. *Biore-sour. Technol.* 2011, 102, 2897–2903.
- [97] Kristensen JB, Felby C, Jørgensen H. *Appl. Biochem. Biotech-nol.* 2009, 156, 557–562.
- [98] Roche CM, Dibble CJ, Knutsen JS, Stickel JJ, Liberatore MW. *Biotechnol. Bioeng.* 2009, 104, 290–300.
- [99] Mohanram S, Amat D, Choudhary J, Arora A, Nain L. *Sustain. Chem. Process.* 2013, 1, 15–27.
- [100] Ye Z, Zheng Y, Li B, Borrrusch MS, Storms R, Walton JD. *PLoS One* 2014, 9, e109885.
- [101] Viikari L, Alapuranen M, Puranen T, Vehmaanperä J, Siika-aho M. *Adv. Biochem. Eng. Biotechnol.* 2007, 108, 121–145.
- [102] D'Amore T, Stewart GG. *Enzyme Microb. Tech.* 1987, 9, 322–330.
- [103] Chu BCH, Lee H. *Biotechnol. Adv.* 2007, 25, 425–441.
- [104] Jeffries TW. *Curr. Opin. Biotechnol.* 2006, 17, 320–326.
- [105] Dien BS, Cotta MA, Jeffries TW. *Appl. Microbiol. Biotechnol.* 2003, 63, 258–266.
- [106] Ballesteros M, Oliva JM, Negro MJ, Manzanares P, Ballesteros I. *Process Biochem.* 2004, 39, 1843–1848.
- [107] Shaw AJ, Podkaminer KK, Desai SG, Bardsley JS, Rogers SR, Thorne PG, Hogsett DA, Lynd LR. *Proc. Natl. Acad. Sci.* 2008, 105, 13769–13774.
- [108] Karimi K, Emtiazi G, Taherzadeh MJ. *Enzyme Microb. Tech.* 2006, 40, 138–144.
- [109] Kim TH, Taylor F, Hicks KB. *Biore-sour. Technol.* 2008, 99, 5694–5702.
- [110] Ko JK, Bak JS, Jung MW, Lee HJ, Choi I-G, Kim TH, Kim KH. *Biore-sour. Technol.* 2009, 100, 4374–4380.
- [111] Zhu S, Wu Y, Yu Z, Zhang X, Wang C, Yu F, Jin S, Zhao Y, Tu S, Xue Y. *Biosyst. Eng.* 2005, 92, 229–235.
- [112] Pimenova NV, Hanley TR. *Appl. Biochem. Biotechnol.* 2004, 113–116, 347–360.
- [113] Stickel JJ, Knutsen JS, Liberatore MW, Luu W, Bousfield DW, Klingenberg DJ, Scott CT, Root TW, Ehrhardt MR, Monz TO. *Rheol. Acta* 2009, 48, 1005–1015.
- [114] Knutsen JS, Liberatore MW. *J. Rheol.* 2009, 53, 877–892.

- [115] Wiman M, Palmqvist B, Tornberg E, Lidén G. *Biotechnol. Bioeng.* 2011, 108, 1031–1041.
- [116] Dasari RK, Berson RE. *Appl. Biochem. Biotechnol.* 2007, 136–140, 289–299.
- [117] Viamajala S, McMillan JD, Schell DJ, Elander RT. *Bioresour. Technol.* 2009, 100, 925–934.
- [118] Bennington CPJ, Kerekes RJ, Grace JR. *Can. J. Chem. Eng.* 1990, 68, 748–757.
- [119] Ehrhardt MR, Monz TO, Root TW, Connelly RK, Scott CT, Klingenberg DJ. *Appl. Biochem. Biotechnol.* 2010, 160, 1102–1115.
- [120] Rosgaard L, Andric P, Dam-Johansen K, Pedersen S, Meyer AS. *Appl. Biochem. Biotechnol.* 2007, 143, 27–40.
- [121] Knutsen JS, Liberatore MW. *Energy Fuels* 2010, 24, 6506–6512.
- [122] Samaniuk JR, Scott TC, Root TW, Klindenberg DJ. *J. Rheol.* 2012, 56, 649–665.
- [123] Pimenova NV, Hanley TR. *Appl. Biochem. Biotechnol.* 2003, 105–108, 383–392.
- [124] Palmqvist B, Lidén G. *Biotechnol. Biofuels* 2012, 5, 57–66.
- [125] Sakata M, Ooshima H, Harano Y. *Biotechnol. Lett.* 1985, 7, 689–694.
- [126] Roche CM, Dibble CJ, Stickel JJ. *Biotechnol. Biofuels* 2009, 2, 28–39.
- [127] Dasari RK. High-solids saccharification and viscosity studies in a scraped surface bio-reactor. PhD Thesis. 2004.
- [128] Mais U, Esteghlalian AR, Saddler JN. *Appl. Biochem. Biotechnol.* 2002, 98–100, 463–472.
- [129] Ingesson H, Zacchi G, Yang B, Esteghlalian AR, Saddler JN. *J. Biotechnol.* 2001, 88, 177–182.
- [130] Samaniuk JR, Scott CT, Root TW, Klingenberg DJ. *Bioresour. Technol.* 2011, 102, 4489–4494.
- [131] Palmqvist B, Wiman M, Lidén G. *Biotechnol. Biofuels* 2011, 4, 10–18.
- [132] Lenting HBM, Warmoeskerken MMCG. *J. Biotechnol.* 2001, 89, 217–226.
- [133] Riedlberger P, Brüning S, Weuster-Botz D. *Bioprocess Biosys. Eng.* 2013, 36, 927–935.
- [134] Aden A, Ruth M, Ibsen K, Jechura J, Neeves K, Sheehan J, Wallace B, Montague L, Slayton A, Lukas J. Lignocellulosic biomass to ethanol process design and economics utilizing co-current dilute acid prehydrolysis and enzymatic hydrolysis for corn stover. *Technical Report NREL/TP-2002, 510-32438, NREL.*
- [135] Hoyer K, Galbe M, Zacchi G. *J. Chem. Technol. Biotechnol.* 2009, 84, 570–577.
- [136] Riedlberger P, Weuster-Botz D. *Bioresour. Technol.* 2012, 106, 138–146.
- [137] Solomon J, Elson TP, Nienow AW, Pace GW. *Chem. Eng. Commun.* 1981, 11, 143–164.
- [138] Elson TP, Cheesman DJ, Nienow AW. *Chem. Eng. Sci.* 1986, 41, 2555–2562.
- [139] Amanullah A, Hjorth SA, Nienow AW. *Chem. Eng. Sci.* 1998, 53, 455–469.
- [140] Dasari RK, Dunaway K, Berson RE. *Energy Fuels* 2009, 23, 492–497.
- [141] Jørgensen H, Vibe-Pedersen J, Larsen J, Felby C. *Biotechnol. Bioeng.* 2007, 96, 862–870.

Bionotes



Bohdan Volynets

Bohdan Volynets has obtained his Bachelor of Engineering (Honors) in chemical engineering from Ryerson University, Toronto, Canada. He has been awarded the Chemical Institute of Canada Silver Medal for academic excellence in undergraduate studies. Bohdan is currently pursuing graduate studies in chemical engineering at Ryerson University. His thesis is on mixing of lignocellulosic biomass for cellulosic ethanol production application.



Farhad Ein-Mozaffari

Farhad Ein-Mozaffari received his PhD in chemical engineering from the University of British Columbia. Currently, he is a Professor in the Department of Chemical Engineering at Ryerson University. Dr. Ein-Mozaffari is a registered professional engineer in Ontario, Canada. His research interests are mixing, computational fluid dynamics (CFD), flow visualization (e.g. tomography and ultrasonic velocimetry), multiphase flow, non-Newtonian fluid flow, hydrodynamics of bioreactors, discrete element modeling (DEM), CFD-DEM coupling, and powder blending.



Yaser Dahman

Yaser Dahman has a research focus on several emerging areas of technology in the fields of biotechnology, nanotechnology, with a special interest in biomedical engineering. He has commissioned a state-of-the-art research facility at Ryerson to conduct his research projects, which were funded by several national agencies. His research activities evolved into the production of biofuels from renewable resources such as agricultural crops and wastes in addition to algae. He is actively involved in developing and testing new types of bioreactors that are mainly utilized in fermentations and other biotechnology applications.